IMPROVED RADAR RANGE-GATED MTI PROCESSOR

Charles James Boyle

NAVAL POSTGRADUATE SCHOOL
Monterey, California

THESIS

IMPROVED RADAR RANGE-GATED MTI PROCESSOR

by

Charles James Boyle

December 1975

Thesis Advisor: David B. Hoisington

SECURITY CLASSIFICATION OF THIS PAGE (When Data Entered)

REPORT DOCUMENTATION PAGE		READ INSTRUCTIONS BEFORE COMPLETING FORM
1. REPORT NUMBER	2. GOVT ACCESSION NO.	3. RECIPIENT'S CATALOG NUMBER
4. TITLE (and Subtitle) Improved Radar Range-Gated MTI Processor		5. TYPE OF REPORT & PERIOD COVERED Master's Thesis December 1975
		6. PERFORMING ORG. REPORT NUMBER
7. AUTHOR(s) Charles James Boyle		8. CONTRACT OR GRANT NUMBER(s)
9. PERFORMING ORGANIZATION NAME AND ADDRESS Naval Postgraduate School Monterey, California 93940		10. PROGRAM ELEMENT, PROJECT, TASK AREA & WORK UNIT NUMBERS
11. CONTROLLING OFFICE NAME AND ADDRESS Naval Postgraduate School Monterey, California 93940		12. REPORT DATE December 1975
		13. NUMBER OF PAGES 91
14. MONITORING AGENCY NAME & ADDRESS(if different from Controlling Office) Naval Postgraduate School Monterey, California 93940		15. SECURITY CLASS. (of this report) Unclassified
		15a. DECLASSIFICATION/DOWNGRADING SCHEDULE

16. DISTRIBUTION STATEMENT (of this Report)

** Approved for public release; distribution unlimited.

17. DISTRIBUTION STATEMENT (of the abstract entered in Block 20, if different from Report)

18. SUPPLEMENTARY NOTES

19. KEY WORDS (Continue on reverse side if necessary and identify by block number)

20. ABSTRACT (Continue on reverse side if necessary and identify by block number)

A redesigned timing circuit and improved bandpass filters were constructed and integrated with the MTI range-gate-and-filter modification kit for the Naval Postgraduate School AN/UPS-1D radar. Principle improvements allow operation in a jittered PRF mode and increased effectiveness of channel filters through the use of active fifth-order Butterworth analog filters. The design objectives were to achieve the

DD FORM 1 JAN 73 1473 EDITION OF 1 NOV 65 IS OBSOLETE
(Page 1) S/N 0102-014-6601 |

SECURITY CLASSIFICATION OF THIS PAGE (When Data Entered)

SECURITY CLASSIFICATION OF THIS PAGE(When Data Entered)

elimination of blind speeds, improved frequency response of the channel filters and the reduction of the MTI minimum discernable signal.

Improved Radar Range-Gated MTI Processor

by

Charles James Boyle
Captain, United States Marine Corps
B.S., Pennsylvania State University, 1969

Submitted in partial fulfillment of the
requirements for the degree of

MASTER OF SCIENCE IN ELECTRICAL ENGINEERING

from the

NAVAL POSTGRADUATE SCHOOL
December 1975

ABSTRACT

A redesigned timing circuit and improved bandpass filters were constructed and integrated with the MTI range-gate-and- filter modification kit for the Naval Postgraduate School AN/UPS-1D radar. Principle improvements allow operation in a jittered PRF mode and increased effectiveness of channel filters through the use of active fifth-order Butterworth analog filters. The design objectives were to achieve the elimination of blind speeds, improved frequency response of the channel filters and the reduction of the MTI minimum discernable signal.

TABLE OF CONTENTS

LIST OF TABLES

LIST OF ILLUSTRATIONS

ACKNOWLEDGEMENT

The author wishes to express his great appreciation and thanks to his wife Pat. Without her considerable effort and skill as an editor and computer programmer, this thesis would not have been produced by the "Text Processing System" on the Naval Postgraduate School's IBM 360 computer.

A special thanks is owed to Mr. Ross Seely, Radar laboratory Supervisor, for his suggestions and advice during the design of the circuitry and his technical expertise and support during the testing phase.

Finally a large measure of the success of this thesis belongs to Professor David B. Hoisington for his ideas, technical proficiency, general support and encouragement throughout the entire effort.

I. INTRODUCTION

For most doppler radars the main objective is to detect moving targets, in the presence of non-moving ones, on the basis of their inherent doppler frequency shift. This doppler frequency shift may be used to enhance the visibility of moving targets when compared to non-moving targets. Moving-target- indication (MTI) radars employ the doppler shift, in an otherwise conventional pulse radar, to increase this visibility. The MTI improvement factor is a figure of merit for an MTI system. It is a power ratio defined as $I = R_O/R_I$, where R_O and R_I are the target-to-clutter ratios at the output and input to the receiver, averaged over all target speeds. This definition allows for both the clutter attenuation of the MTI system and the variation of gain of the MTI system with target velocity. It is therefore a measure of the MTI system's ability to improve the target-to-clutter ratio.

Discrimination between fixed and moving targets is obtained by determining the change in phase of successive echoes from a given target in a sequence of pulses. Any target moving with a relative radial velocity with respect to the radar location will present a frequency shift in the reflected signal, and hence a progressive change of phase. The relationship that describes the doppler frequency shift is given by

$$F_D = 2V_R/\lambda$$

F_D = Doppler frequency shift

V_R = Relative (radial) velocity of the target with respect to the radar location.

λ = radar wavelength

If F_D is in hertz, V_R in knots, and λ in centimeters

$$F_D = 103V_R / \lambda$$

It is usually the case that fast moving targets such as aircraft, ships and land vehicles have higher radial velocities relative to a fixed radar than do stationary or near stationary targets such as terrain, clouds, sea water, vegetation, etc. Obviously the clutter (both fixed and slow moving targets) can be reduced by providing, for each element cf range, some method of frequency discrimination such as a bandpass filter that will effectively eliminate undesired frequency components and preserve the desired ones.

The filtering may be accomplished after heterodyning in the receiver the carrier frequency to zero frequency. Pulse signals in the video amplifier of the radar will be unmodulated in amplitude for fixed targets, and modulated at the doppler frequency for moving targets as shown in Figure 17.

However, there are complicating factors present that must be taken into account. First, all returned signals are amplitude modulated by the radar antenna. In effect, the spectrum of all signals, including clutter, is spread out by an amount depending on antenna beamwidth and rotaticn speed. Therefore the clutter spectrum is not concentrated entirely at zero frequency but is spread over a finite band of low frequencies. Second, certain clutter signals such as vegetation and ocean waves have additional frequency spread due to incidental motion. This additional frequency spread

is, primarily, a function of the type of clutter and wind velocity. Therefore, because of the finite bandwidth of clutter return, it is desirable that the clutter filter eliminate a band of frequencies about zero frequency. Ideally the width of this rejection band should be adjustable to accomodate a range of antenna rotation rates and a range of clutter characteristics.

The transmitted spectrum of a pulse radar consists typically of some thousands of components on each side of the carrier frequency with a spacing equal to the pulse repetition frequency. Each line of the received spectrum suffers from spreading due to the two effects mentioned above. In addition the lines of the received spectrum of a moving target are all shifted by the doppler frequency. If the frequency components are translated by subtracting the carrier frequency, a typical video spectrum associated with clutter and one moving target at a particular range is obtained as shown in Figure 1.

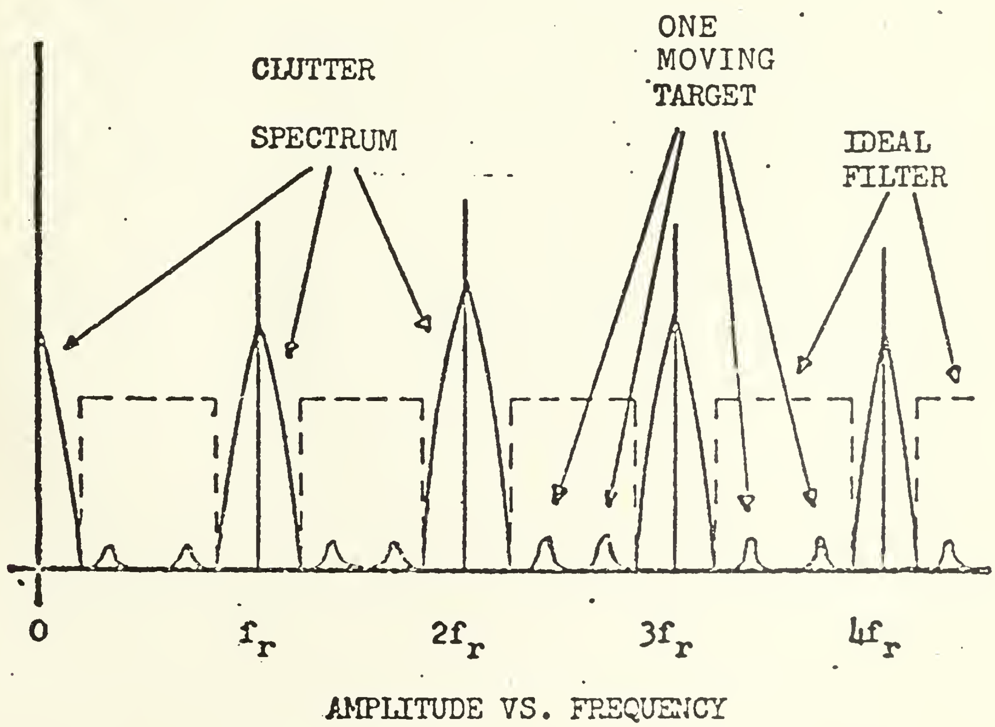

Figure 1. Pulse-radar video spectrum.

One method of eliminating the clutter spectrum is then to employ a comb filter with a transmission characteristic as shown by the dashed lines.

The traditional method of obtaining a comb filter is to use a delay-line canceler. A second method with several inherent advantages is to employ range gates with bandpass filters. These methods are discussed in the next section.

II. MOVING-TARGET INDICATORS

A. DELAY-LINE CANCELERS

In an MTI delay-line canceler the bipolar video signal is delayed an amount equal to the pulse period and subtracted from an undelayed signal as shown in Figure 2. Video pulse signals from moving targets are amplitude modulated at the doppler frequency or, for $F_D > F_R/2$ at $|F_D \pm NF_R|$, where N is an integer, F_R = pulse repetition frequency, F_D = doppler frequency, and the value of N is such that the modulation frequency is between 0 and $F_R/2$. The successive pulse returns from the fixed targets have constant amplitude, except for variation due to antenna scanning and incidental clutter motion. Successive pulse echoes from any given target are separated in time by the pulse repetition period of the radar in use. Since successive fixed target clutter signals are nearly identical, clutter is very materially reduced by the canceler. For moving targets pulse-to-pulse cancellation normally does not occur since successive pulses generally are of different amplitude.

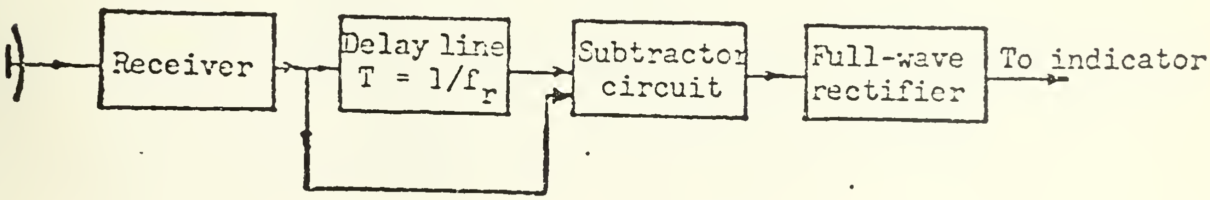

Figure 2. Single delay-line canceler.

Although the single delay-line canceler is simple in concept it does not show the characteristics of an ideal comb filter. The frequency transfer characteristic may be shown to be in the form of a rectified sine wave as indicated by the solid curve of Figure 3.

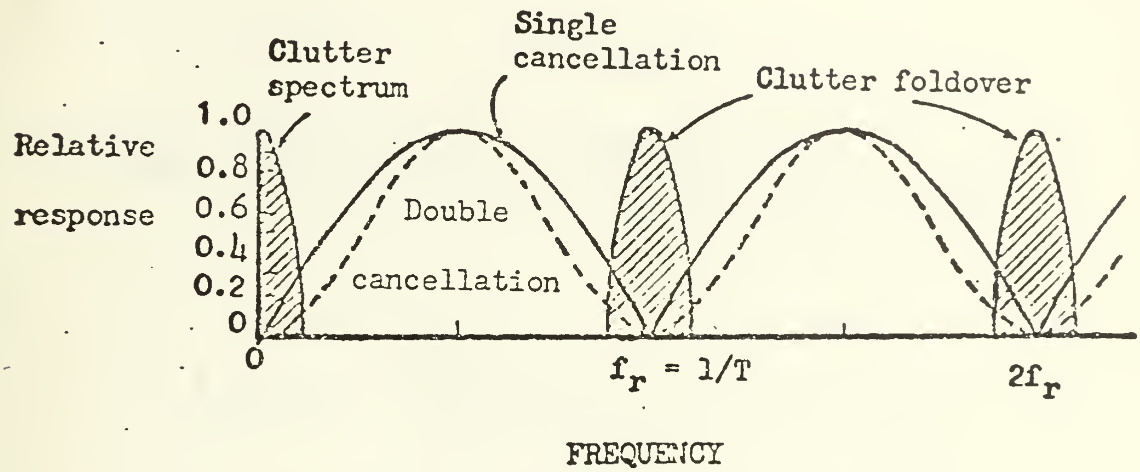

Figure 3. Characteristic response of a DLC.

If the moving target doppler frequency shift is equal to any multiple of the pulse repetition frequency, then $(NF_R - F_D) = 0$ and cancellation occurs as for fixed targets. A target speed which causes this effect, with the doppler shift equal to any multiple of the pulse repetition frequency, is called a blind speed, where $F_D = 2V_R/\lambda = NF_R$. The relationship implies the target's doppler frequency is in the nulls of Figure 3's cancellation curves.

Conventional pulse radars employ pulse periods in the order of 1000 usec or more, so this relatively long delay is required of the delay line. To provide a delay of this magnitude an acoustic delay line is generally used.

To improve clutter cancellation, double delay-line cancelers can be used, see Figure 4. The frequency response

of the double delay-line canceler is shown in dashed lines in Figure 3. The main drawbacks of the double delay-line cancelers are the cost, the complexity, and the size of such a system, and the fact that the filter characteristics are still far from ideal. Improved frequency response can be obtained by using multiple delay lines at greatly increased complexity.

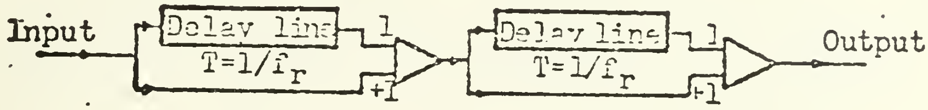

Figure 4. Double delay-line canceler

The basic disadvantages of delay-line cancelers are high insertion loss of the delay line (35 to 70 dB), temperature dependence of delay, a very tight tolerance on line delay which must be held within a very small fraction of the pulse width, the tendency to introduce some spurious signals due to multiple reflections, degradation of signal-to-noise ratio, amplitude variation of moving-target echoes due to the variation of gain with frequency, complexity, and complete breakdown of the system if there is a failure of any one of many elements in the system. Since the delay time is fixed when the delay line is constructed, this also fixes the pulse repetition frequency of the radar. This prevents the use of a variable PRF to eliminate blind speeds unless delay lines of different lengths are employed.

The employment of different length delay lines implies multiple or staggered PRF's, which require careful consideration of the effect of second-time-around echoes. In the case of a staggered PRF, second-time-around target

echoes do not have the same time relationship at the input to the delay-line canceler, and an uncanceled residue results just as if the target were in motion. Moreover, a second-time-around echo will appear at two different ranges.

B. RANGE-GATED MTI

MTI by range-gating and filtering (RGF) is another method of implementing a moving-target indicator system. This method gives greatly improved frequency response as compared to a delay-line canceler, and vastly improved reliability. The main disadvantage has been the circuit complexity, large size, high power consumption, and the cost of the system. The advent of semiconductor technology and subsequent micro-miniaturization has helped to overcome these obstacles, and has opened new methods of investigation and research in this area.

As has been seen, any moving target has a doppler frequency component equal to or less than half the pulse repetition frequency in the video amplifier. Hence a bandpass filter with a lower cut-off frequency above the maximum clutter frequency and an upper cut-off frequency equal to half the PRF of the radar might well be used to pass the doppler information while eliminating fixed target clutter. There are important limitations to this technique.

First, by its nature the narrow-band filter degrades the range information contained in the return signal. Second, signals from moving targets at all ranges could enter the filter.

Range gates may be employed to separate target echoes on the basis of their different times of arrival for different ranges. Signals in the various range gates may then be applied to separate filters. Range information is therefore

not lost, and interference between targets at different ranges is eliminated. A bandpass filter follows each range gate to eliminate clutter while passing signals due to moving targets.

There are important advantages to this scheme over the delay-line canceler. Since large numbers of channels are operated in parallel, if any one of them fails very little information is lost. Overall system reliability is high. Cancellation of clutter can be achieved by using more nearly ideal filters since greater flexibility of filter design is available for simple bandpass filters than for comb filters. With special integrated circuits a range-gated MTI radar should be no longer physically larger nor consume more power than an MTI radar employing a delay-line canceler. It should be relatively easy to eliminate blind speeds with range-gated MTI by using random pulse repetition periods, while with delay-line cancelers it is difficult to use even two pulse repetition periods, and this only partially eliminates blind speeds.

Several range-gated MTI radars have been built at different locations. Although there has been much difference in detail, the basic operation has been the same for all.

III. OBJECTIVES

The prime objective was to improve the performance of an existing 20 channel range-gated MTI processor, which was designed and constructed by Koral [Ref. 1]. Three areas of possible improvement were selected

1. Elimination of blind speeds
2. Improved frequency response of the channel filters
3. Reduction of MTI minimum discernable signal

The first area of consideration suggested a variable PRF, ideally a random PRF. The second and third areas seemed to indicate a detailed analysis of the bandpass filter in the range-gated channels would lead to methods to produce the desired results. The first task was to design, build and test a reliable, digital timing circuit to provide the basic radar trigger at a pre-determined PRF, and the synchronization required to provide gating pulses for the existing 20 range-gated channels. Once this was accomplished, the circuitry was modified to allow a random pulse period with precisely the same pre-determined average PRF as in the jitter-free case while maintaining full synchronization with the channel gating pulses. By selecting the gate pulse width to be less than the inverse of 2 times the video bandwidth of the AN/UPS-1D complete preservation of all video information is maintained. To accomplish this a pulse width less than 0.666 usec is required.

The detailed analysis of the existing Sallen-key, analog filter was obtained through modeling with the network analysis program NASAP. The results revealed that little if any improvements in the band-reject region could be achieved

by changing values of the components, and attempts to reduce the number of filter elements only degraded the frequency response. Instead a active fifth-order Butterworth analog filter was obtained commercially, and interfaced with the existing range-gated channels. This implementation was an attempt to both improve the characteristics in the band-reject region and reduce the physical size of the filter.

In an attempt to savalage as much of Koral's [Ref. 1] work as possible, all five of the sample-and-hold/video reconstructor printed circuit boards were used, as well as the basic packaging he constructed. The integration of the new timing scheme and new filter boards was accomplished by using, with minor modifications, the existing wiring scheme and circuit board receptacles and locations. The power distribution system was redesigned and rewired with filtering on all four values of DC voltage required. All solid state components and integrated circuits were used.

Some characteristics of the AN/UPS-1D radar are given in Table 1.

AN/UPS-1D Air Search Radar

PRF (Hz)	Pulse Width (usec)	Antenna Pattern	Antenna Rotation Rate	Carrier Frequency	Pulse Power
800	1.4	Horizontal 3 dB beamwidth of 2.5 degrees	Adjustable up to 15 RPM.	1300MHz (λ = 23 cm)	1.4Mw Typically

Table 1. Some characteristics of AN/UPS-1D air search radar

Because of the impracticality of constructing sufficient channels for full MTI operation at all radar ranges within time and cost restraints, only 20 channels were implemented. The timing circuit was designed, constructed, tested and interfaced with the existing 20 channels. One filter board with four Butterworth filters was designed, constructed and tested, then the balance of the 20 filters were installed.

In the next section, system description and experimental procedures are discussed in detail.

IV. SYSTEM DESCRIPTION, DESIGN AND OPERATION

The system block diagram is shown in Figure 5. Bipolar video containing both coherent (non-moving) and non-coherent (moving) targets, is taken directly from the AN/UPS-1D's receiver and applied as the input to the range-gated MTI processor (i.e. to each of the 20 channels). The outputs of these channels are combined to form a reconstructed video signal for the one mile range interval covered by these 20 channels. The range interval may be placed at any range from zero to maximum range.

In the test system the video signal may be evaluated and compared with that obtained through the parallel delay- line canceler in the AN/UPS-1D. The resulting signal (MTI Video) is displayed on a PPI scope. The timing circuitry provides radar trigger at an 800 Hz PRF in the non-jittered mode, and at an average 800 Hz PRF in the jittered mode. In addition the timing circuit provides successive gating pulses to the channels in synchronization with the radar PRF for both jittered and non-jittered modes so that one channel after the other is enabled in turn. The width of each pulse is nominally 0.625 microseconds to insure maximum extraction of information contained in the sampled video signal (i.e. want sampling rate to be greater than bandwidth of radar receiver IF stage which is 1.5 MHz).

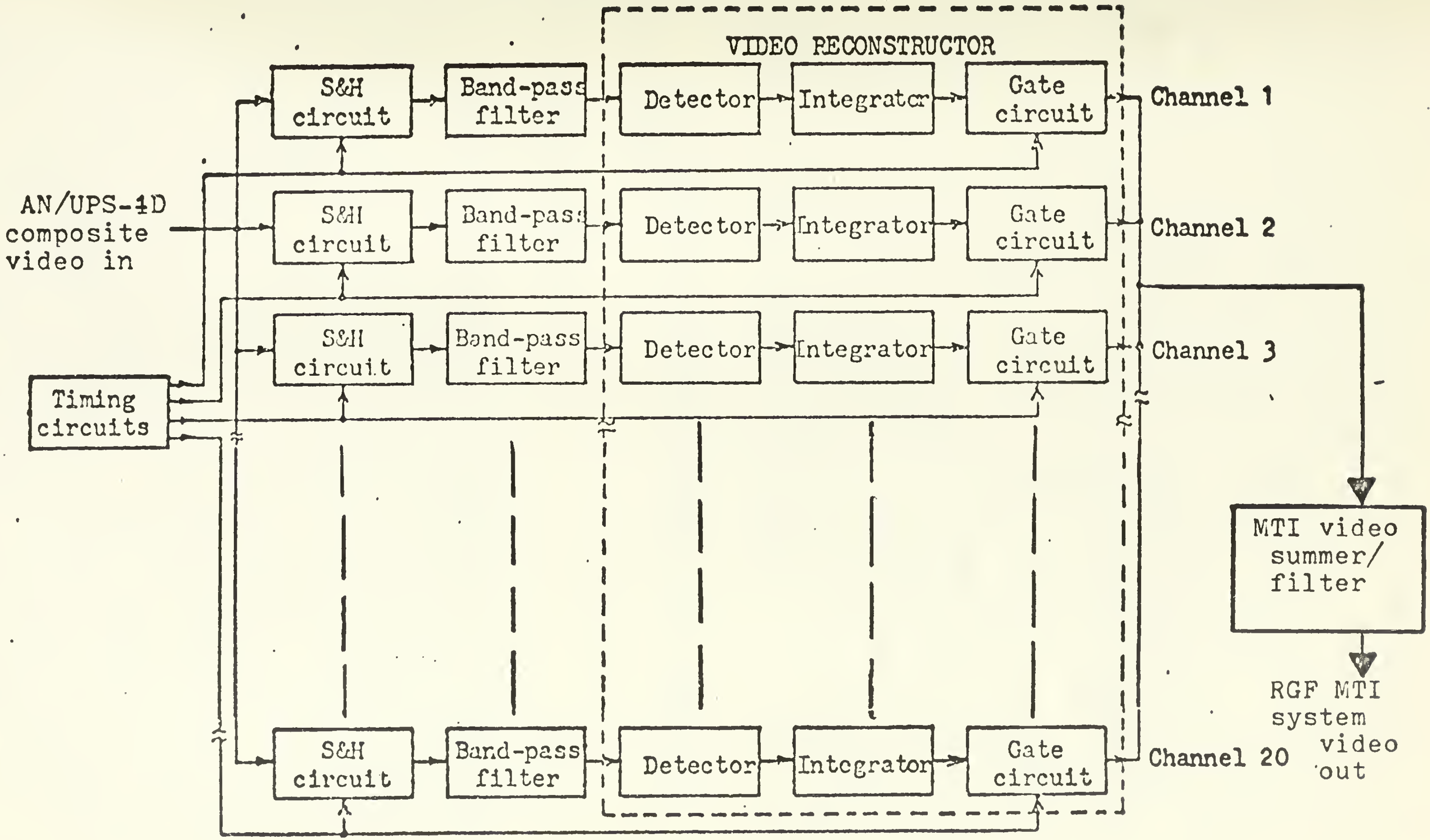

Figure 5. MTI by range gates and filters, block diagram

The master oscillator used in conjunction with a pulse shaping circuit produces pulses at a 1.6128 MHz rate with spacing between the pulses equal to the pulse width (i.e. symmetrical square wave). Thus successive channels receive a portion of the input video signal corresponding to successive range intervals. The desired range interval is selected by setting the required amount of delay, provided by the Tektronix 546 oscilloscope delay unit, to the trigger which initiates the "loading" of the shift registers that provide the basic gates, see Figure 6. Therefore each channel contains, for a short range interval, target, clutter and noise information. This signal is filtered to eliminate clutter, rectified, integrated, and a pulse formed to represent the amplitude of the remaining signal at that specific range interval. By summing the outputs of all the channels the nearly clutter-free MTI video signal is obtained, and displayed on a scope.

The following sections discuss the individual circuits in detail.

A. TIMING CIRCUIT

Basic requirements determining the design of the timing circuitry are as follows. The first was to provide a radar trigger and an adjustable delay after this trigger before the first range gate is enabled. The second requirement was to achieve a jittered PRF with the average value equal to the basic (800 Hz) PRF while maintaining full synchronization with the range-gating scheme. The third was that the design be such that the circuit can easily be extended to include many additional channels with very high stability and reliability. The adjustable delay was obtained through the variable delay unit in a Tektronix 546 oscilloscope which can be pre-set to allow operation at the specific range (time) required. To accomplish the remainder

of the requirements integrated circuits were used throughout the entire design except that one 2N2907A transistor was used to get sufficient trigger amplitude to "fire" the AN/UPS-1D's transmitter. The overall timing system block diagram is shown in Figure 6.

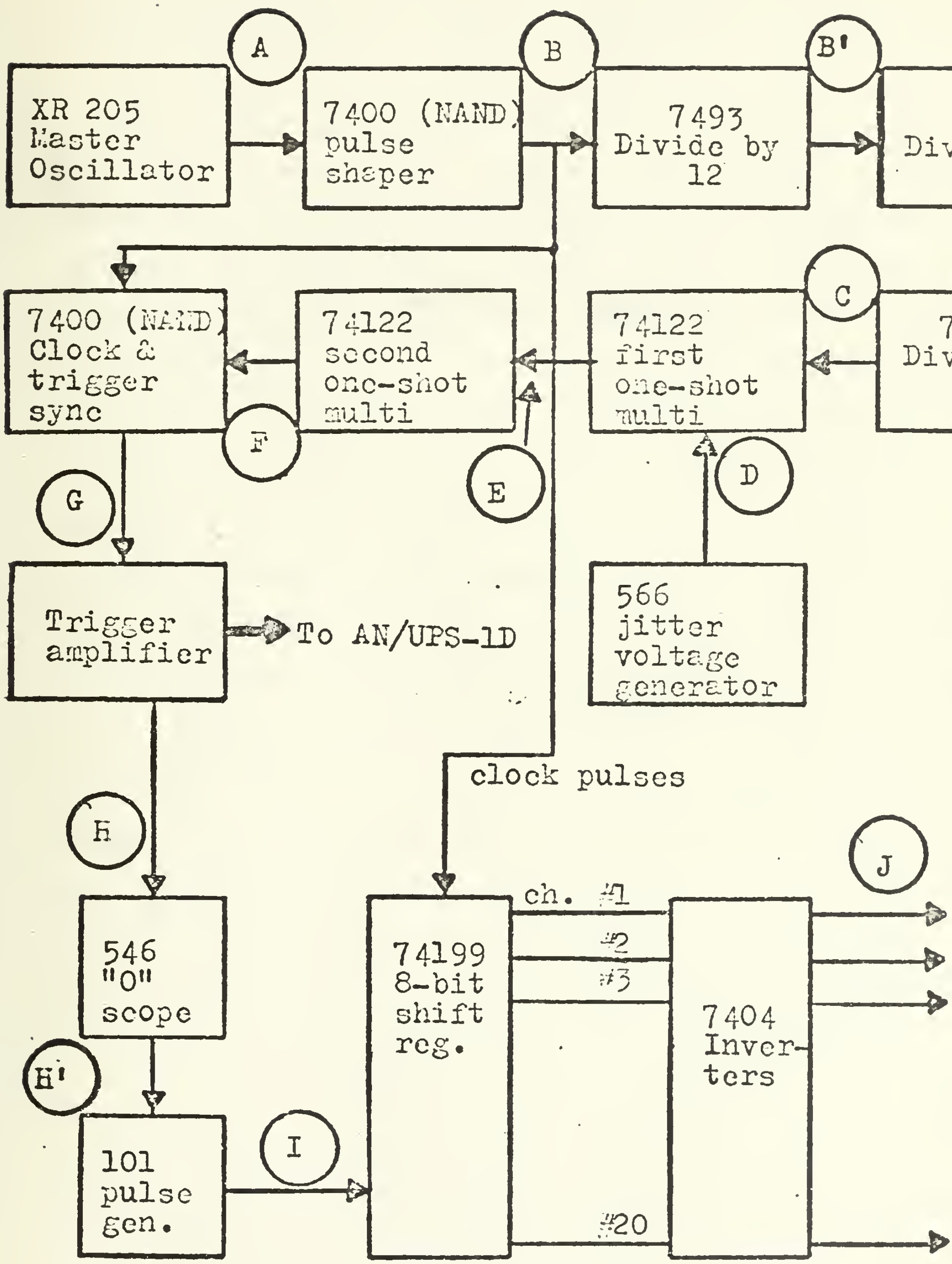

Figure 6. Block diagram of timing circuit.

Full specifications on all devices may be obtained in References 5 through 8. Photographs of the waveforms at Points A through J of Figure 6 are depicted in Appendix A. Circuit diagrams are shown in Appendix C.

The XR205, monolithic waveform generator, was used as the R-C controlled master oscillator (clock pulse generator). At Point A of Figure 6 a slightly distorted "sinusoidal" output at a very stable frequency of f_o = 1.6128 ± 0.00015 MHz is obtained, see Figure 27. This sinusoidual wave is shaped into a symmetrical square wave, at frequency f_o, T = 0.620 usec. The now formed clock pulses at Point B of Figure 6 are fed to two locations, to Point F on the system block diagram, which will be discussed later, and to the first of three frequency dividing circuits. The waveforms at B and the output of the first divide-by-twelve are shown in Figure 28. The waveform as it subsequently divided by the second divide-by-twelve and finally by the divide-by-fourteen is shown in Figures 29 and 30 respectively. At this point, (C), the trailing edge (or down clock) of the now 800 Hz square wave triggers a one-shot multivibrator, see Figure 31. The one-shot remains high for approximately 1125 usec then returns to the low or zero level, see Figure 31. There is another input to this first one-shot and it is a 980 KHz square wave from a NE566 Waveform Generator, see Figure 36. This generator delivers a 5 volt peak-to-peak waveform varying at a 980 KHz rate to the V_{CC} pin of the 1st one-shot. This has the effect of varying the bias point internally in the 74122 integrated circuit, which produces an output waveform that has a high level varying in time at the same 980 KHz rate. The final result is that the trailing edge or down clock of the 1st one-shot has a varying period of 1000 usec to 1500 usec, but maintains an average period of 1250 usec (800 Hz, the basic PRF required for the AN/UPS-1D). The results are depicted in Figures 32 and 35.

The requirement for triggering the AN/UPS-1D call for a +20V, 1.4 usec pulse at an 800 Hz rate. Therefore the output at Point E is fed to a second one-shot to obtain a 0.5 usec pulse, see Figures 33 and 34. This 0.5 usec pulse is gated with the original pulse stream (at frequency f_o) frcm Point B to insure that the radar trigger and any one of the clock pulses are time synchronous, see Figure 37. The idea here is that the clock pulses used to step the shift registers, which are generating the required range-gated channel gating pulses, must be time synchronized with the delayed radar trigger. The delayed radar trigger is used as the serial data input or initial loading of the 1st shift register. Thus insuring the first range-gated pulse is in time synchronization with the radar trigger that has fired the radar transmitter. To achieve the required trigger for the AN/UPS-1D the output at G, shown in Figure 37 as a negative 5v pulse, is fed to the base of a transistor amplifier, cutting the device off and producing a +22v approximately 1.2 usec wide pulse at an 800 Hz average rate to trigger the AN/UPS-1D transmitter, see Figures 38 and 40.)

The trigger used to fire the AN/UPS-1D transmitter is simutaneously fed to the Tektronix 546 oscilloscope, delayed in time as desired, then fed to a Syntron-Donner pulse generator to reduce the amplitude and reshape the pulse, see Figure 41. This processing allows a time synchronous trigger to be used as the serial data input to the 1st shift register. The delayed trigger loads with a logical "1" the 1st shift register and the clock pulses (at frequency f_o) cause this logical "1" to be shifted at the clock rate to produce the basic gating pulses. The 8th output of the 1st shift register is fed to the second shift register as the serial data input, which also has the same clock pulse train input. Therefore extendtability is inherent in that cascading registers, all clocked from the same source,

implies that once the 1st register is loaded with a logical "1" the registers will continue to shift from the 1st to last, restricted only by the number of registers cascaded and the power sources available.

The parallel outputs of the shift registers are inverted, as depicted in Figure 35, to provide successive gating pulses for each channel. The output of each channel is a 0.625 usec wide, negative 5 volt pulse which is used as the gating pulse for the corresponding sample-and-hold and video reconstructor circuits. Each successive gate pulse is one pulse width delayed from the previous one so that equal gate intervals are provided. The waveforms at important points in the timing circuit are sketched in Figure 7.

Four supply voltages are required for the MTI circuits, +24,-24,+5,-5 volts.

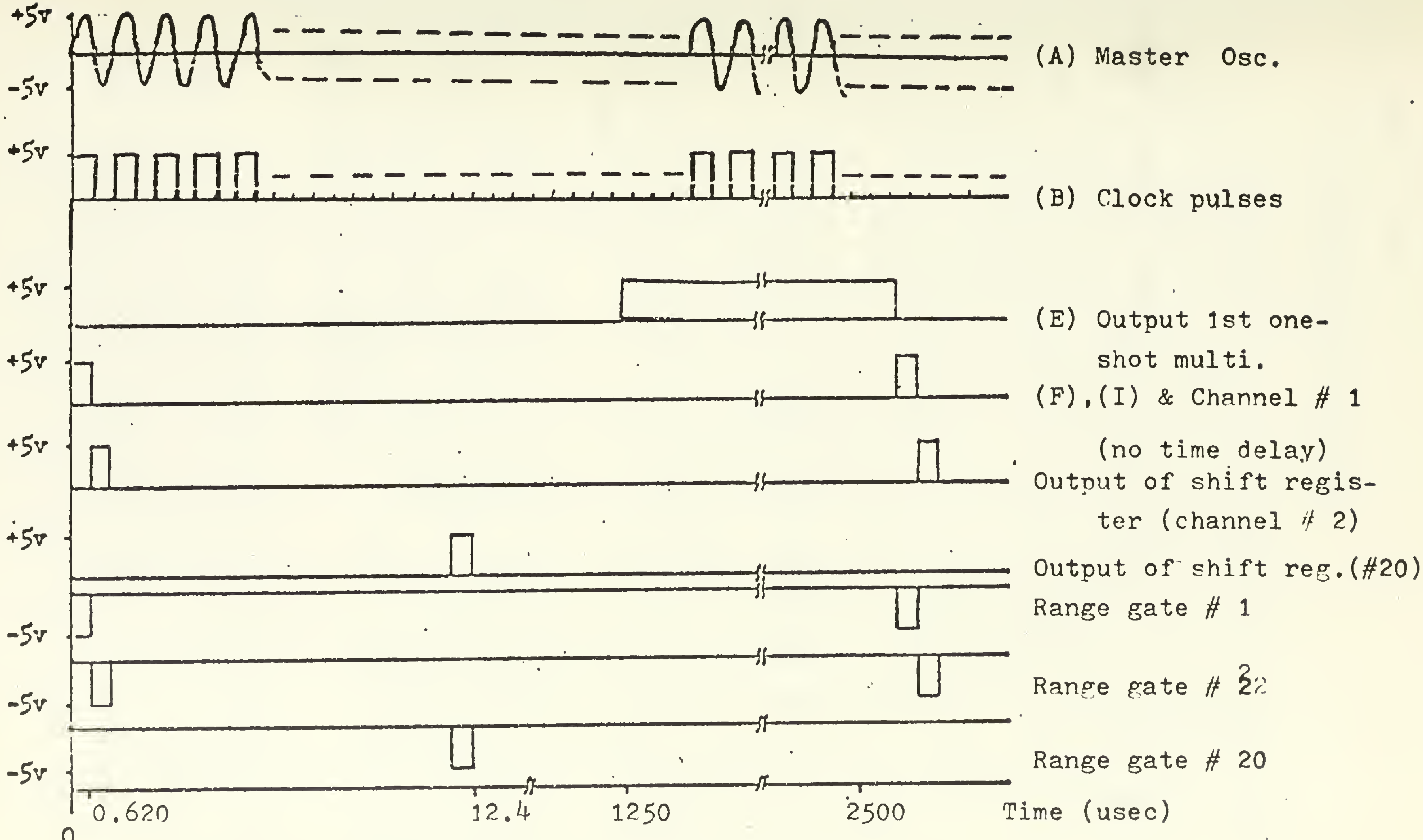

Figure 7. Waveforms in the timing circuit.

B. RANGE GATES

1. Sample-and-hold Circuit

The purpose of the sample part of the sample-and-hold circuits is to separate the video signal into range (time) increments, thus allowing transmission through a narrow-band filter without any loss of range information. This process is called range-gating. The width of the range gates is a function of several interrelated factors. The first is range accuracy required. This in turn is related to the IF bandwidth and to the complexity which can be tolerated. Video bandwidth in conventional pulse radars is generally greater than half the IF bandwidth so that the system bandwidth is determined in the IF amplifier. Therefore, as previously stated, a gate width of 0.625 usec was established to allow the sampling rate to be greater than the IF amplifier bandwidth. It should be noted that a gate interval of this size allows full utilization of the inherent range resolution capability of the radar. Range resolution is limited by the transmitted pulse width, not by the gate width.

The sample of video signal is held on a capacitor for one pulse repetition period. The reason for holding the sample is that by stretching the pulse to the full period the lowest frequency component is emphasized, while the high-frequency components, which carry no significant information, are suppressed.

For proper operation of the circuit, the charging time constant should be less than the width of the sampling pulse so that there will be adequate time to charge the hold capacitor to the signal level during the sampling period. This necessitates a gate with very low resistance when on. The resistance should be very high when not sampling. A

small hold capacitor can then be used to minimize the time constant.

One of the most important criteria in choosing a gate was to obtain a circuit which would operate essentially with zero offset voltage. In other words the gating pulse itself should not appear as a pedestal at the output.

The other important point was to obtain gate operation with short sampling times. Switching times in the low nanosecond range were necessary.

All transistors, diodes, and FET's used in construction of the unit are high-speed, low-switching-time devices.

The circuit diagram of the sample-and-hold circuit is shown in Figure 8.

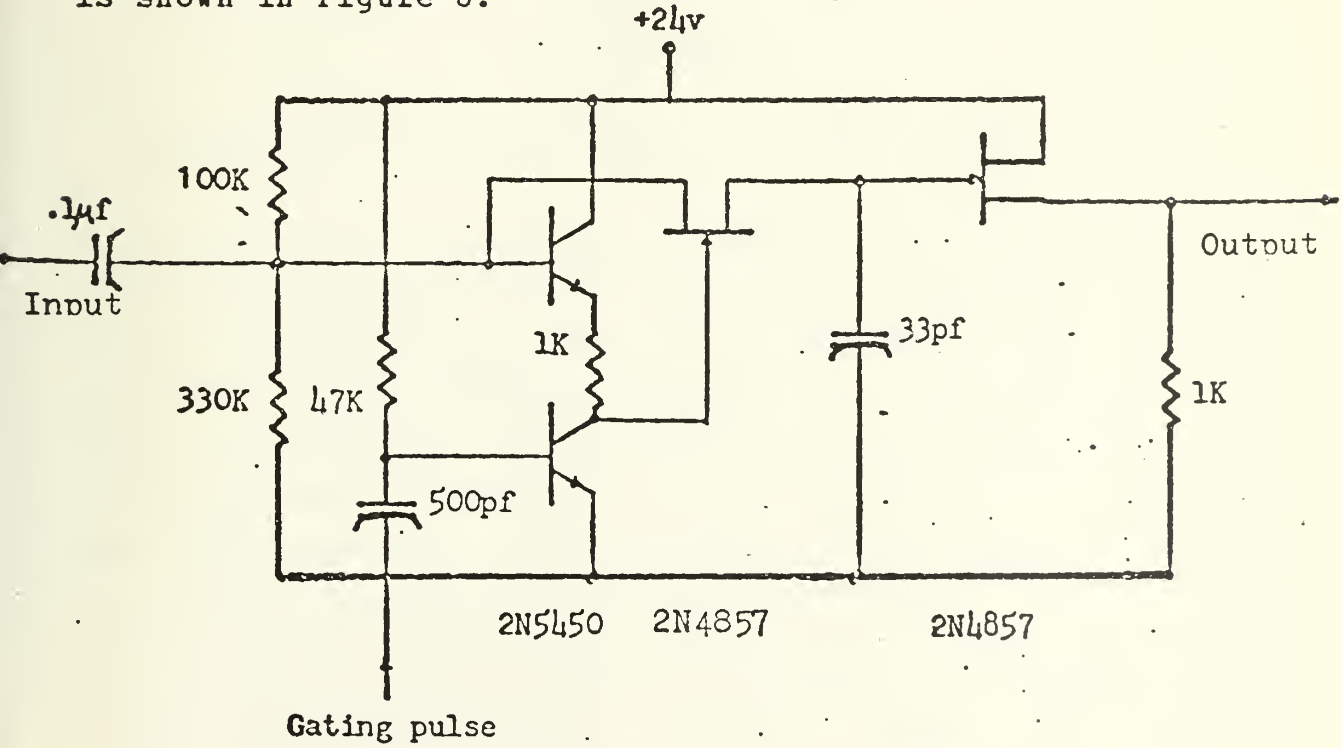

Figure 8. Sample-and-hold circuit.

2. Filter circuit

The heart of the range-gated system is the bandpass filter which allows the doppler frequencies from moving targets to pass, but which eliminates the DC and low doppler frequencies of fixed and slow moving targets.

The desired frequency response of the filter is shown in Figure 9.

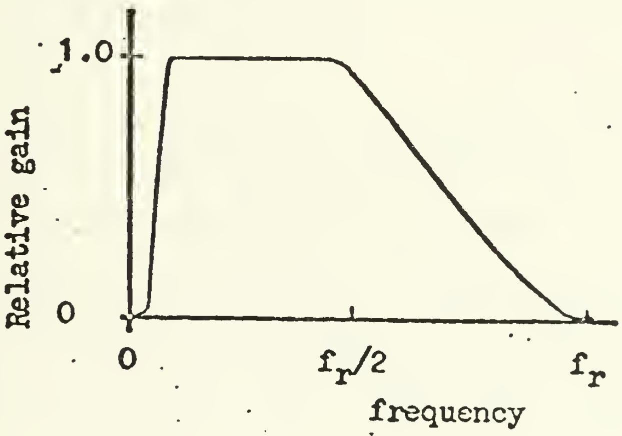

Figure 9. Frequency response of the bandpass filter.

The lower cut-off frequency should be just above the highest clutter frequency. Since the clutter spectrum is not constant due to adjustable speed of rotation of the antenna and to the variation of the spectrum with wind speed and type of scatterers, it is most desirable to make the width of the rejection band adjustable. If this is not possible, selection of the lower cut-off frequency becomes a compromise between elimination of clutter and detection of "slow" moving targets. This is the case here, where F_D = 100 Hz (i.e. $V_R = \lambda F_D/103$ = 22.4 knots) was selected as the lower cut-off frequency. Response should be uniform from the cut-off frequency to one half of the pulse repetition frequency (PRF) of the radar. This is possible, as a result of sampling at the PRF, due to the phenomenon of

frequency aliasing as described in Reference 4. Attenuation should be high at and beyond a frequency equal to the PRF minus the highest clutter component (i.e. 700 Hz in this application).

The filter employed is a commercially obtained active fifth-order Butterworth analog filter, with a bandpass of 100-400 Hz between the 3 dB points. The most critical consideration was to obtain as much attenuation in the band-reject regions as possible while operating with and without a "jittered" PRF.

The experimental response characteristics of this circuit is shown in Section VII, Figure 13 and the connection diagram is in Appendix B. The lower cut-off frequency is 100 Hz while the upper cut-off frequency is 400 Hz between the 3 dB points. The 20 dB rejection bands are from zero to 60 Hz and 740 Hz and above. The (non-jittered) frequency response curve for the sample-and-hold circuit together with the filter is shown in Section VII, Figure 14. Note the zero response at multiples of the PRF. These indicate the blind speeds, (e.g. $V_R = \lambda F_D/103 = 178.6$ knots, where $F_D = 800$ Hz and V_R, are defined on page 11). Inspection of Figure 15 in Section VII indicates the effective elimination of these blind speeds through the application of a jittered PRF, (i.e. the basic PRF of 800 Hz jittered from 600 to 1000 Hz, but averaging 800 Hz, in this case). Multiple valued responses are explained on page 42.

3. Video Reconstructor Circuit

The signal out of the bandpass filter is rectified before integration and video reconstruction. The circuit diagram is shown in Figure 10. The first diode clamps the negative part of the incoming signal at near ground potential. A second parallel diode goes to a small positive

potential through an adjustable resistor. The resistors in the several channels are adjusted to equalize the DC levels at the outputs of the channels.

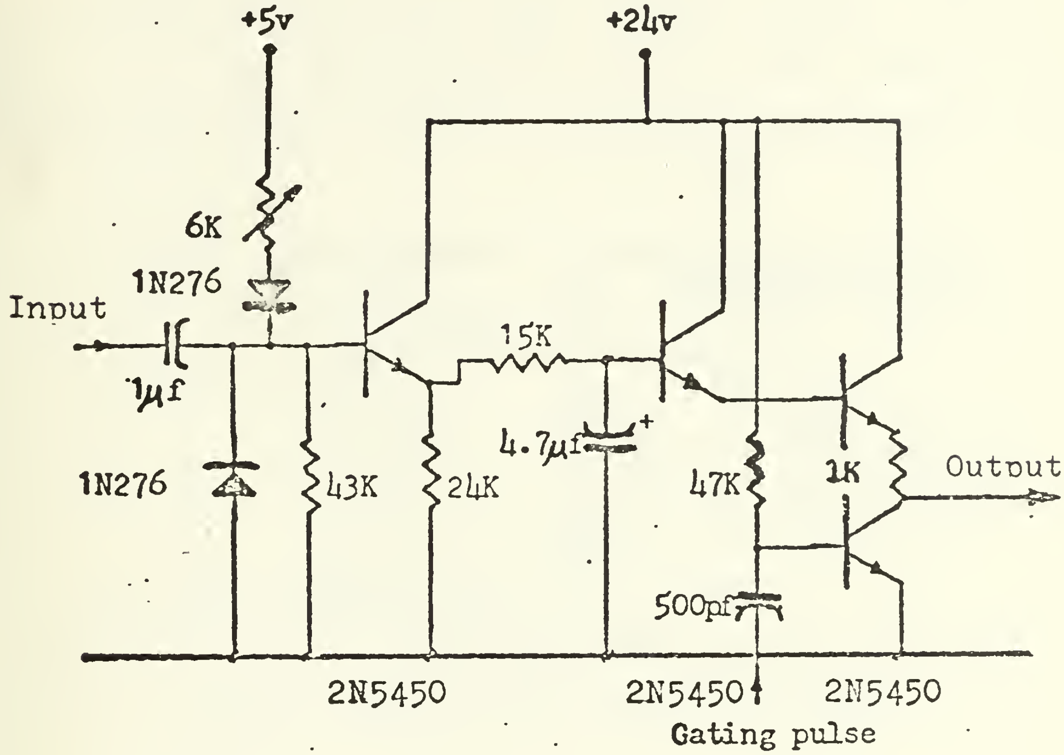

Figure 10. Circuit diagram of rectifier, integrator, and video reconstructor.

This signal is integrated by a R-C low-pass filter after detection. This filter has a time constant comparable to the antenna dwell time on the target (i.e. 75 msec). More efficient integration is therefore obtained than is obtained with the phosphor of a PPI scope. The ability to detect weak signals is therefore enhanced.

The gating pulse which is common to the sample-and-hold circuit and the video reconstructor circuit forms a pulse with amplitude proportional to the integrator output at a time corresponding to the range at which the channel operates with an amplitude proportional to the output of the integrator. A diode is used as the gating

device. Now the signal is reconstructed and is ready to be summed with all other channels and displayed.

The outputs of all video reconstructer circuits are summed and filtered in the MTI video summing network of Figure 11. This R-C integrator with a time constant of 0.7 microseconds helps to smooth the reconstructed video output.

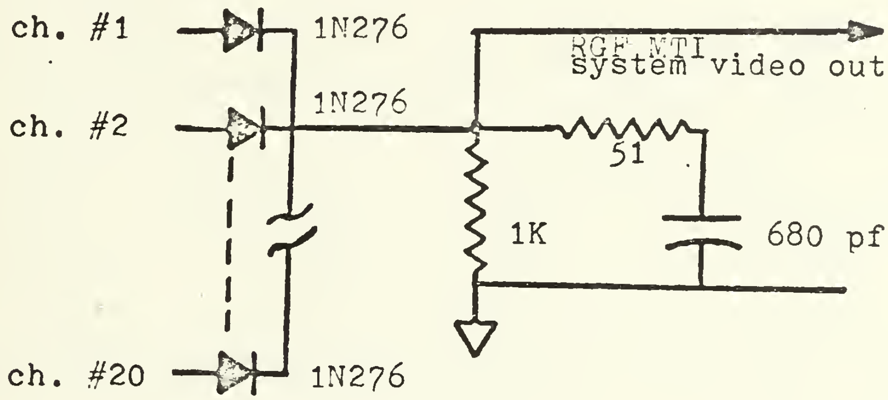

Figure 11. MTI video summer/filter.

V. RANGE-GATED MTI TEST SET-UP

The block diagram for the test set-up is shown in Figure 12.

An SM-65/UP test set was used to generate a coherent (non-moving) target. Figure 17 depicts, on the left, a negative pulse. Positive pulses may be generated by proper selection of the phase selector on the test set. A Ts-419 test set was used to generate non-coherent (moving) target. This target is depicted on the right of Figure 17. Since this target is completely non-coherent it represents a range of velocities. It should be noted that the photo displays the general envelope of the non-coherent target and there are many flucuating phases contained within the envelope as shown in Figure 17. A Hewlet-Packard video amplifier is used as a buffer between the synthetic video output and the input of the range-gated MTI processor. This amplifier serves two purposes, first as isolation between the AN/UPS-1D and the range-gated MTI system and secondly to provide variable gain to the input of the range-gated MTI. A second fixed-gain Hewlet-Packard video amplifier is used to amplify the MTI video output, see Figure 12. Waveforms, at various points were observed and photographed. The experimental data and photographs are presented in the following section.

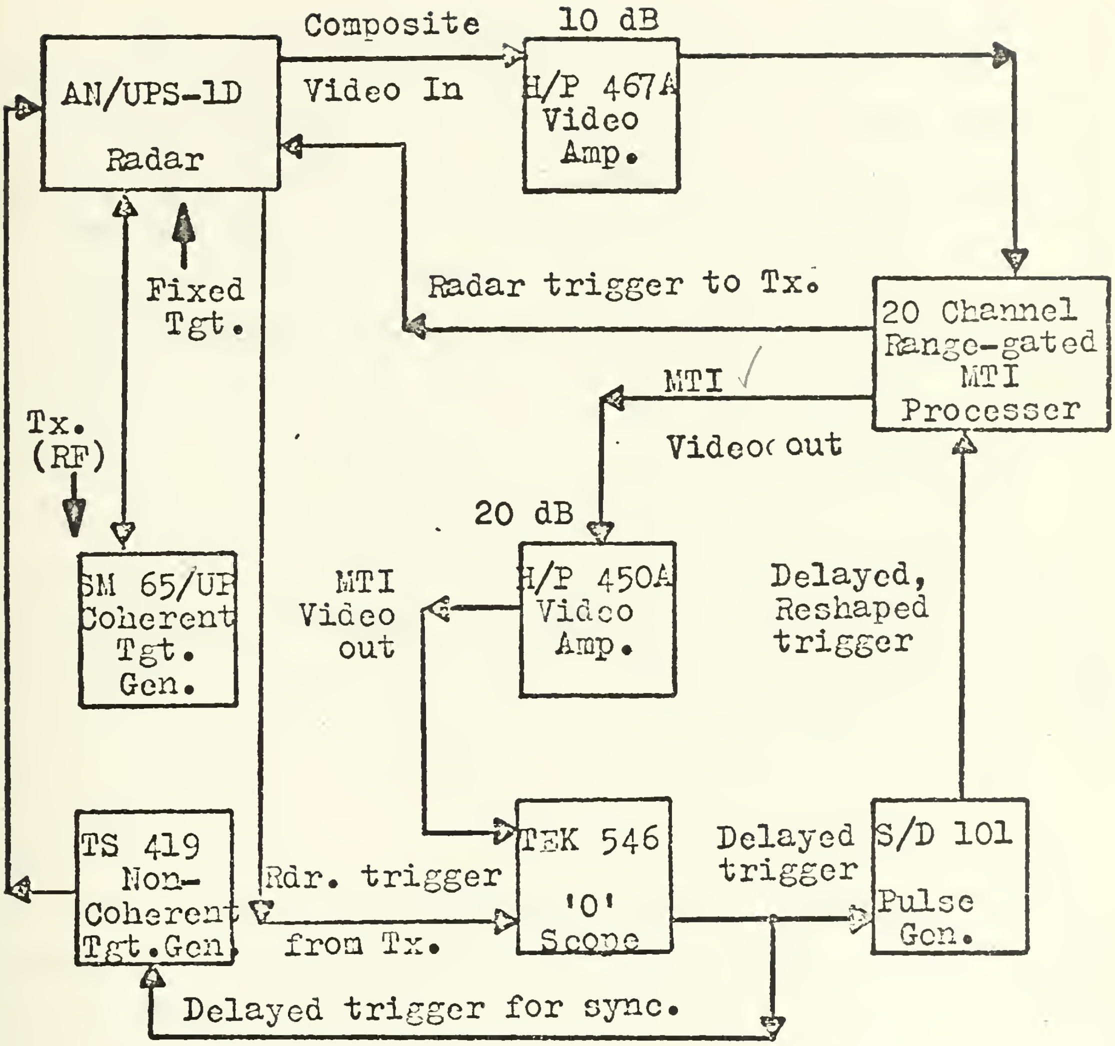

Figure 12. Range-gated MTI test set-up.

VI. RESULTS

To test the range-gate-and-filter combination, one channel consisting of a sample-and-hold circuit (Figure 8), one filter (Section IV and Figure 64), and one video reconstructor (Figure 10) was assembled in breadboard form. The sampling gates were provided by the timing circuitry previously designed and constructed (Section V). The frequency response of the bandpass filter was obtained by applying a sine wave, from a signal generator, directly to the filter input and measuring the magnitude of the DC voltage at the integrator of the video reconstructor (i.e. at the top of the 4.7 microfarad capacitor of Figure 10). Figure 13 is the plot of $|V_{out}|$ vs frequency and represents the frequency response of the bandpass filter (without the sample-and-hold circuit). The ratio of $|V_{out}|$ to $|V_{max}|$ at 50 Hz was 0.06 or -24.4 dB ($20 \log_{10}(0.06) = -24.4$ dB). The ratios at 750 and 800 Hz were -19.2 and -22.0 dB respectively.

Four filters per circuit board were assembled, as diagramed in Figure 64 of Appendix C, and interfaced with the existing channels (i.e. Korals' sample-and-hold and video reconstructor circuit boards, see Figure `65). The connection diagrams are shown in Tables II thru IV of Appendix C.

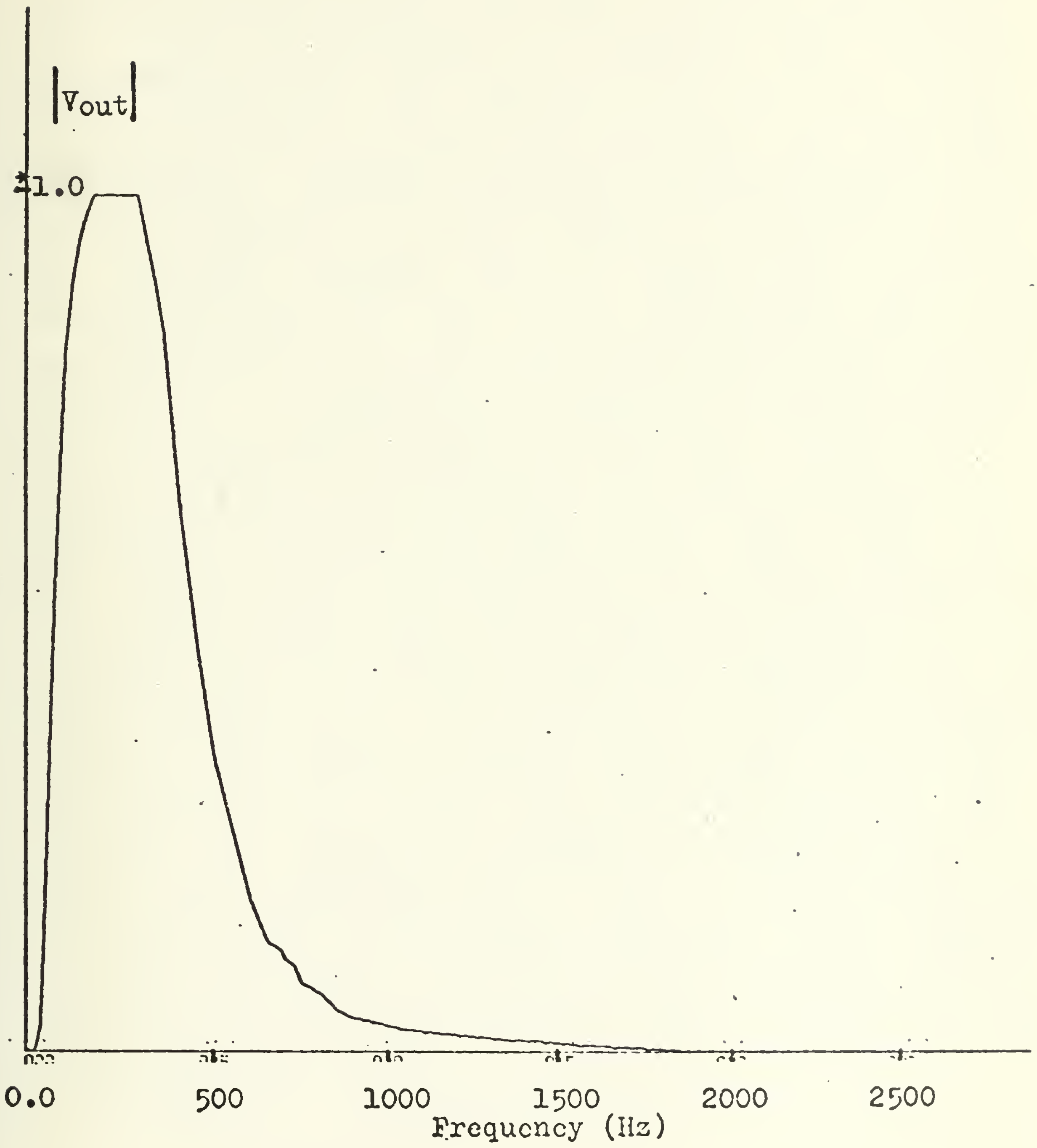

Figure 13. Frequency response of bandpass filter.
(without the sample-and-hold circuit)

Figure 14 represents the frequency response of the cascaded sample-and-hold circuit and bandpass filter. In this case the sinusoidal input was applied to the input of the sample-and-hold, sampled at a constant 800 Hz gating rate, filtered by the bandpass filter and the output measured as the DC voltage at the integrator of the video reconstructor. Frequency aliasing (sometimes referred to as frequency "foldover") with the sampling rate of 800 Hz cause the frequency response curve of Figure 13 to repeat at intervals of 800 Hz, and to be symmetrical about odd multiples of 400 Hz. This effect is completely described in Reference 4. The upper curve in Figure 14 is the maximum value of $|V_{out}|$ and the lower curve is the minimum value of $|V_{out}|$ obtained for a specific frequency. Note these minimum and maximum excursions occur at sub-harmonics of the sampling rate (i.e. 200, 400, 1200, 2000, 2800, etc. Hz). The maximum value occurs when the sampling pulses are coincident with the peak of the signal being sampled and the minimum value when sampling pulses are coincident with the zeroes of the signal. As predicted by Fourier analysis, nulls in the frequency response occur at Nf_s with attenuation bands at $Nf_s \pm 50$ Hz (i.e. 750-850, 1550-1650, 2350-2450 etc. Hz). Using $F_D = 103V_R/\lambda$, as defined on page 11, these nulls correspond to the blind speeds for the non-jittered MTI system operation. The frequency interval, 750-850 Hz, implies, using the above equation with $\lambda = 23$cm and the frequency nulls of Figure 14, that there are blind speeds from 168 to 190 knots, 347 to 369 knots, etc.

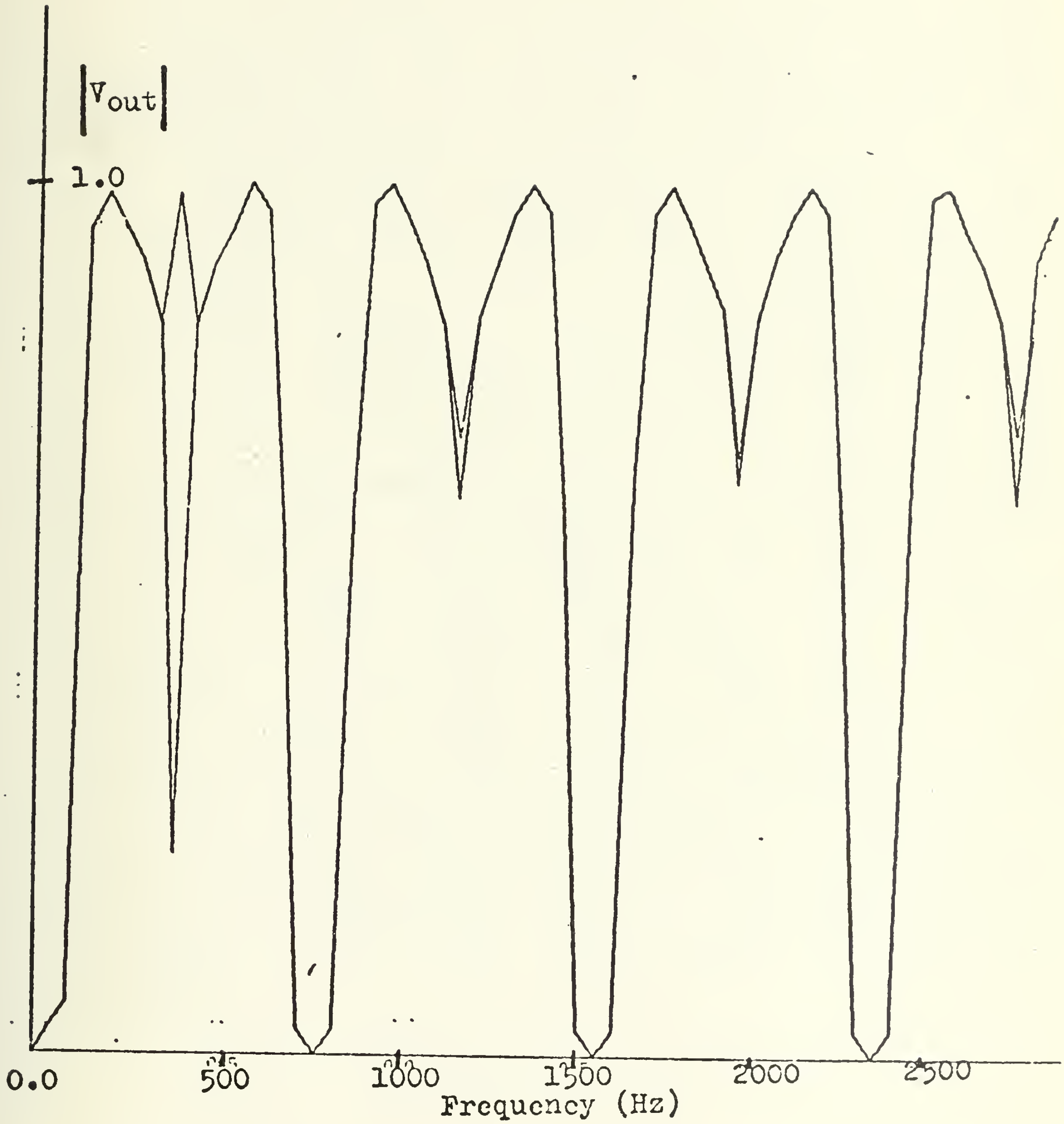

Figure 14. Frequency response of S & H and filter (without PRF jitter).

The final result, Figure 14, represents the frequency response of one channel in the range-gated MTI system with no jitter in the 800 Hz sampling frequency.

Figure 15 represents the frequency response of a range-gated channel when the sampling frequency is jittered. Inspection of Figure 40 of Appendix A reveals that the radar trigger has approximately 500 usec of jitter (i.e. 40% of basic pulse repetition time (PRT) of the AN/UPS-1D). Since the radar trigger and the sample gates are time synchronous, as described in Section IV, the sampling rate is simultaneously jittered at the same frequency and is therefore time synchronous with the radar trigger applied to the AN/UPS-1D. This jittered sample rate causes all nulls but the first of Figure 14 to be filled in and effectively eliminates blind speeds corresponding to a doppler frequency greater than 900 Hz. For doppler frequencies in the 750-850 Hz range the $|V_{out}|$ has increased from zero volts with no jitter to 0.2-0.4 volts (normalized). This is depicted in Figure 15 and indicates that there is a finite probability of detecting targets which have a radial velocity producing doppler frequencies in this range. Experiments using the timing design as described in Section IV revealed that although it was possible to increase the jitter period (i.e. greater than 500 usec), an average pulse period of 1250 microseconds (i.e. PRF 800 Hz) could not be maintained at the larger jitter periods with the circuit employed.

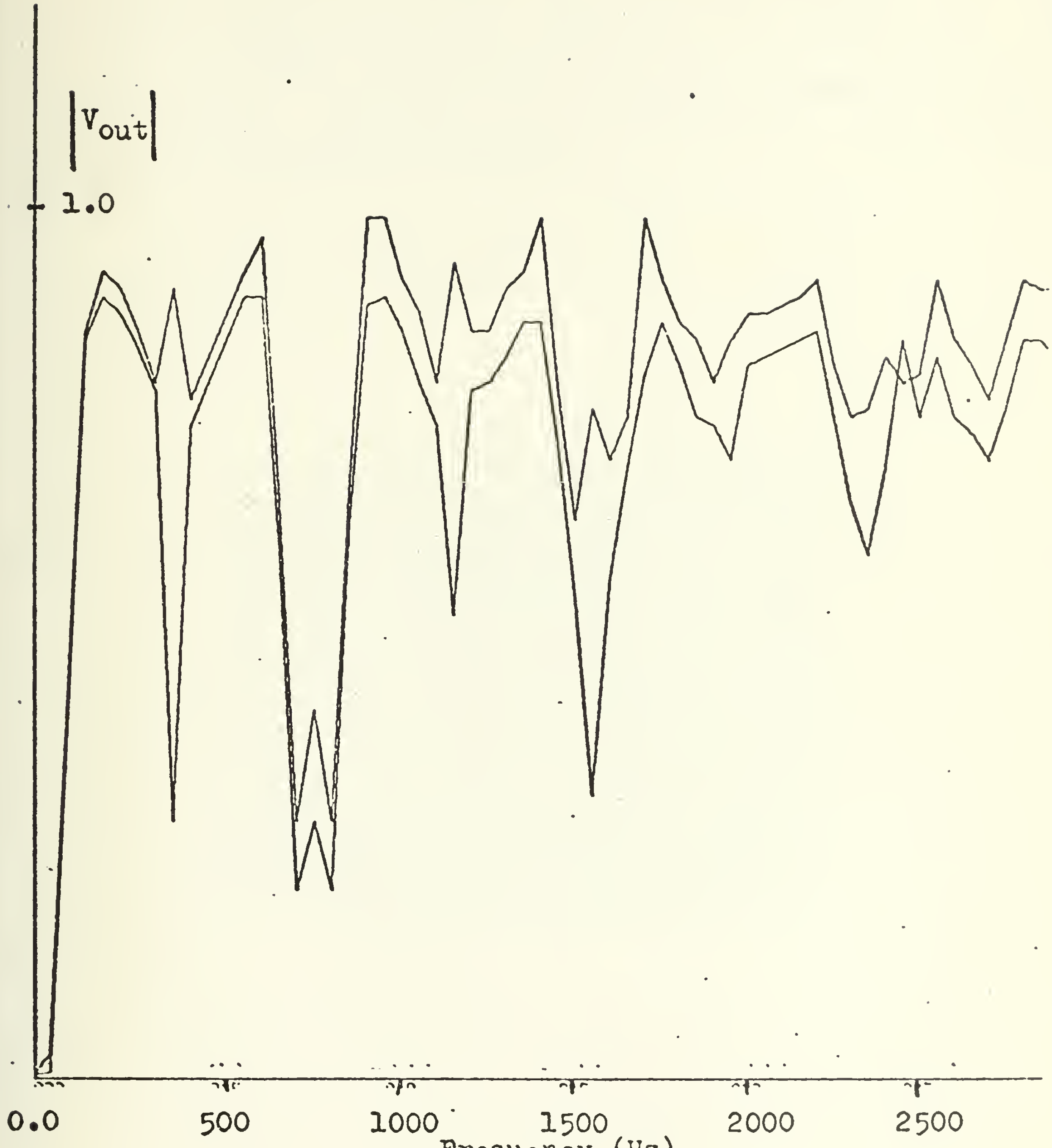

Figure 15. Frequency response of S & H and filter (with PRF jitter).

The system response to simulated video signal of 200 Hz applied tc all 20 channels is shown in Figure 16. The figure demonstrates the uniformity of each cnannels gain with the cverall range-gated MTI system. Figure 17 depicts the bipolar video as obtained from the test set-up (Figure 12) and described in Section V.

The upper trace is the range-gated MTI video output for 20 channels. The lower trace is a 200 Hz sine wave applied as a simulated video input to all channels. The vertical scale is 10 v/cm and the horizontal scale is 2 microseconds/cm.

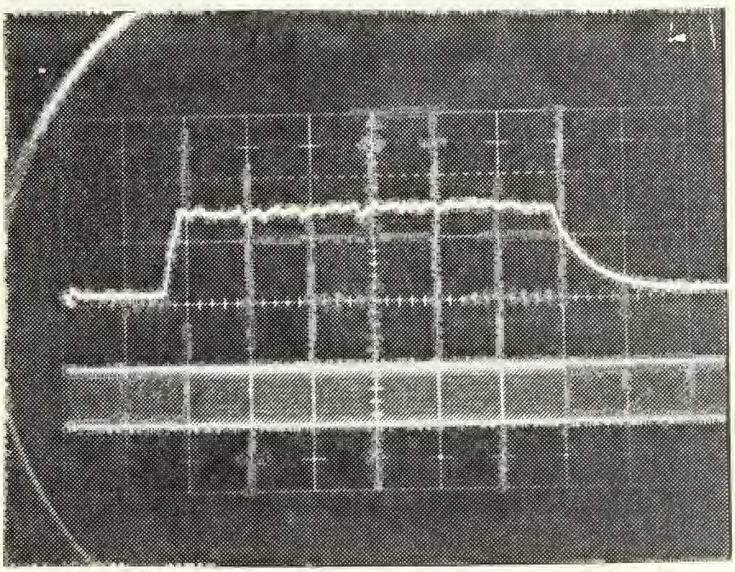

Figure 16. Range-gated MTI video output.

The fixed target which just happens to be a negative pulse, is on the left and the moving target is on the right. The vertical scale is 0.5 v/cm and the horizontal scale is 2 microseconds/cm.

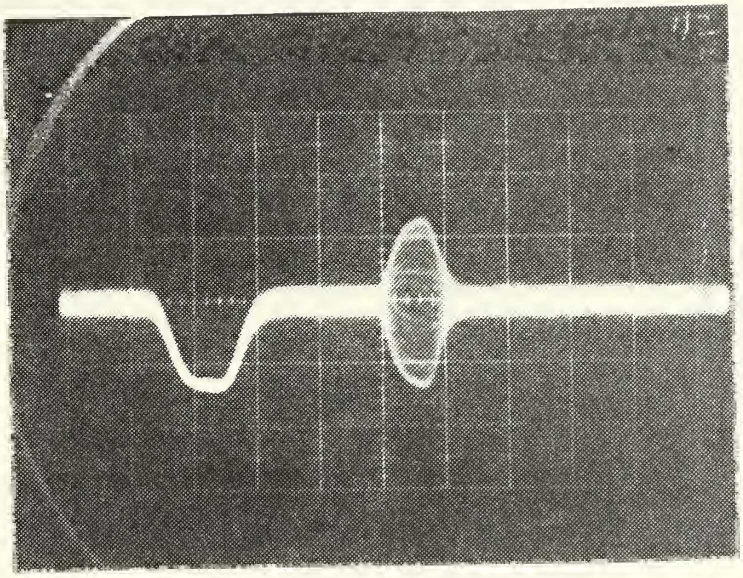

Figure 17. Simulated coherent (fixed) and non-coherent (moving) targets.

The overall system response to these simulated fixed and moving-target echoes is shown in Figures 18 and 19. Note the maximum response is for the moving target (non-coherent, bipolar video) with negligble if any response for the fixed target (which happens to be a negative, coherent video, pulse here). Note also the improvement in the ratio of moving-target signal to noise due to the integrator (i.e. in the video reconstructor (Figure 10)) which averages signal and noise over approximately 56 pulse repetition periods (i.e. the RC time constant of the integrator is 70.5 msec and the average pulse repetition period is 1.25 msec). There is a small dc component in the output of the RGF processor in the absence of any signal. This component increases as input noise level increases. The pedestal seen in Figures 18 and 19 is largely due to processed noise. For a comparison between the range-gated MTI and the AN/UPS-1D's delay-line canceler refer to Figures 20 and 21. While the range-gated MTI offers some response to the heavy clutter (antenna stationary) the greater response to the moving target (bipclar video in upper trace) overcomes the fact that the delay-line canceler shows little response to the clutter and weaker (relative to the range-gated MTI system) response to the moving target.

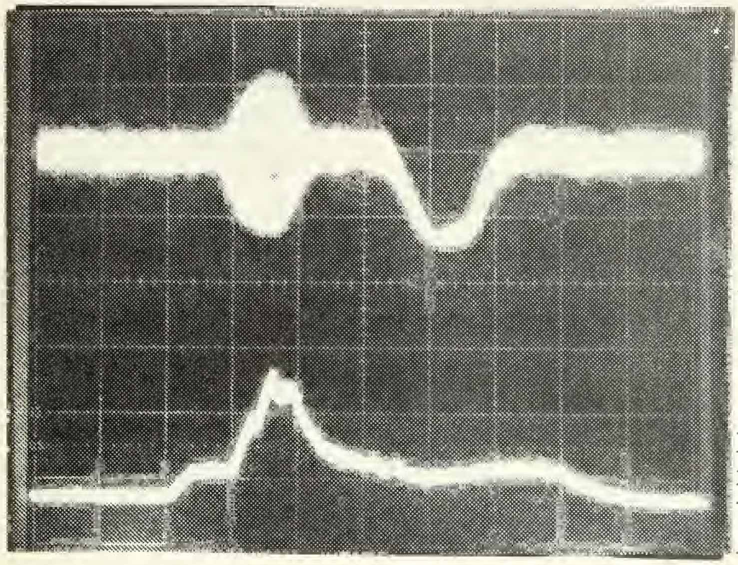

Synthetic target input with vertical scale of 0.5 v/cm

Horizontal scale is 2 microseconds/cm

RGF MTI system response with a vertical scale of 5 v/cm

Figure 18. Range-gated MTI response to the synthetic fixed and moving targets in the MTI range interval concurrently.

Synthetic target input

(same scales as Figure 18)

RGF MTI system output

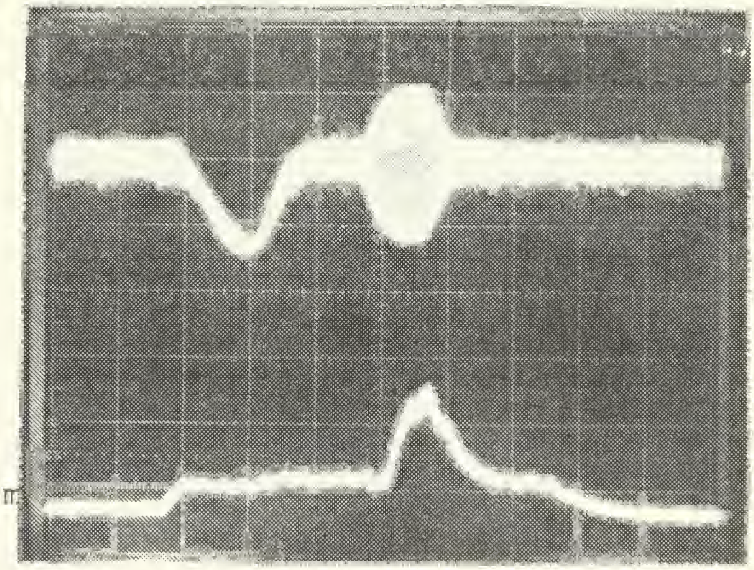

Figure 19. Range-gated MTI response to the synthetic targets which have been interchanged in range (time) with respect to Figure 18.

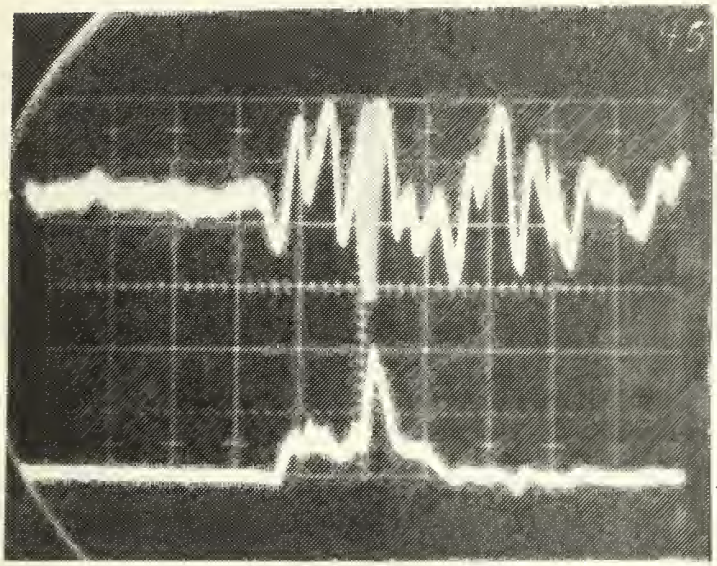

Bipolar video buried in heavy clutter; vertical scale is 0.5 v/cm

Horizontal scale is 5 microseconds/cm

RGF MTI system response with a vertical scale of 5 v/cm

Figure 20. Range-gated MTI system response to a synthetic moving target (bipolar video) buried in heavy clutter. The clutter is from actual fixed targets (antenna stationary).

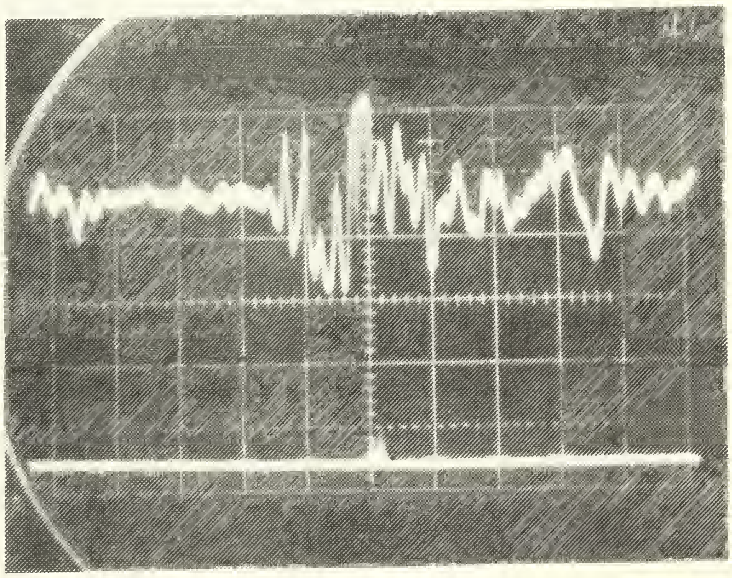

Bipolar video buried in heavy clutter

(same scales as Figure 20)

Delay-line canceler response

Figure 21. AN/UPS-1D delay-line canceler response to a synthetic moving target (bipolar video) buried in heavy clutter. Clutter and signal are approximately the same as in Figure 20 (antenna stationary).

A better comparison between the two systems is the evaluation of minimum discernable signal (MDS), measured in the absence of clutter. The AN/UPS-1D MDS, with the delay-line canceler was measured as -105.1 dBm and is depicted in Figure 22. The response of the range-gated MTI system to a -105.1 dBm target is shown in Figure 23. Note the target is "visible" to the eye (i.e. distinguishable from the noise) in the upper trace and the response in the lower trace is range (time) synchronous with that target. The MDS of the range-gated MTI system was measured to be -109.1 dBm and is shown in Figure 24. There is a definite response on the lower trace, (i.e. the output of the range gates and filters), but the target in the upper trace at the input of the range-gated system is buried in the noise and is not easily discernable. This improvement is due to the improved integration achieved and described on page 49.

The upper trace is the synthetic moving target (bipolar video, no clutter) at -105.1 dBm. The lower trace is the AN/UPS-1D (delay-line cancelter) MTI video output. The vertical scale is 2 v/cm and the horizontal scale is 2 microseconds/cm.

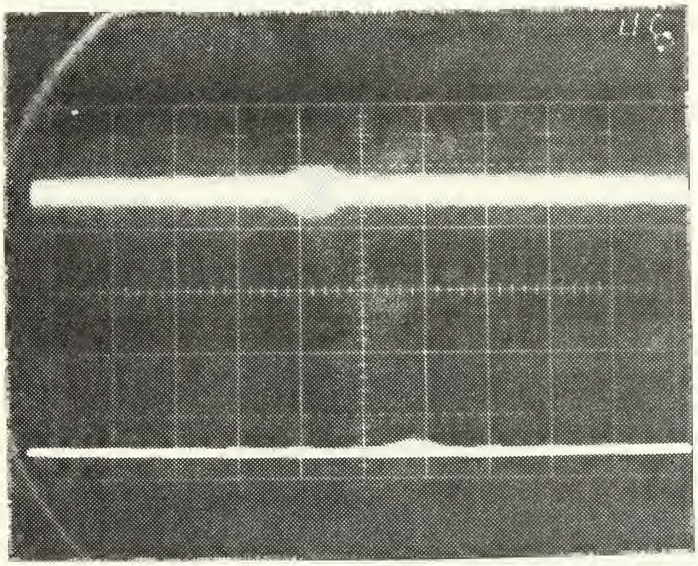

Figure 22. Minimum discernable signal (MDS) of AN/UPS-1D.

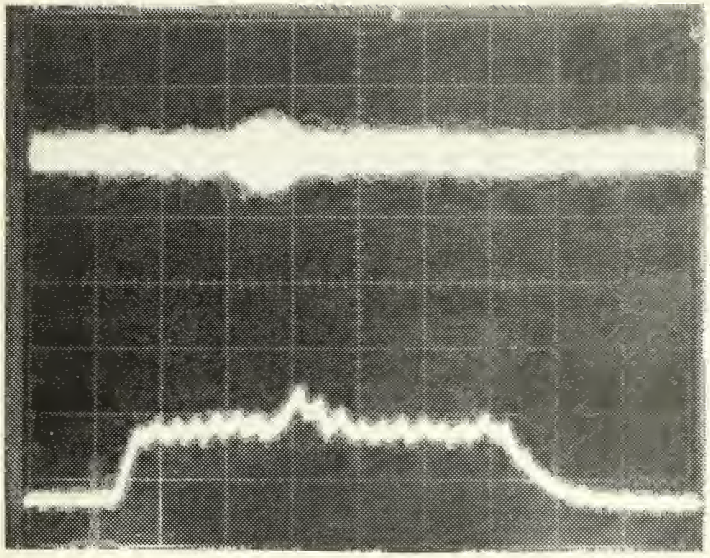

Bipolar video (no clutter) with a vertical scale of 0.5 v/cm

Horizontal scale is 2 microseconds/cm

RGF MTI system response with a vertical scale of 2 v/cm

Figure 23. Range-gated MTI system response to the AN/UPS-1D MDS, (i.e. synthetic moving target at -105.1 dBm and the delay-line canceler by-passed).

Bipolar video (no clutter) at -109.1 dBm

(same scales as Figure 20)

RGF MTI system response

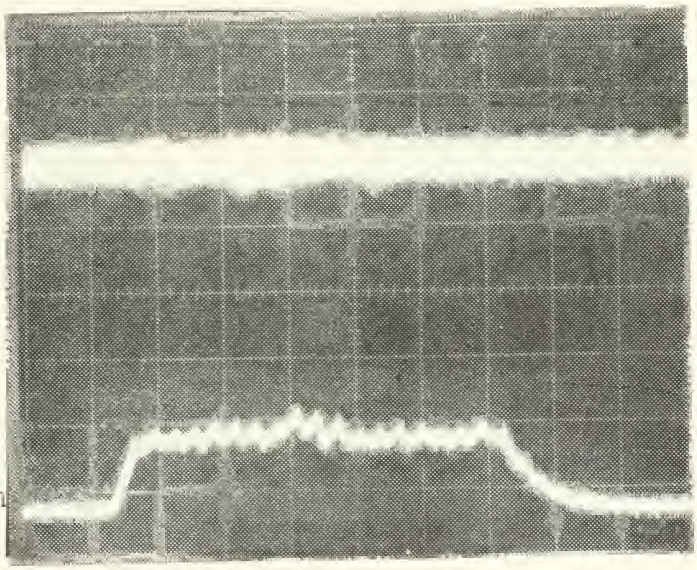

Figure 24. Range-gated MTI system minimum discernable signal (MDS). The delay-line canceler is by-passed.

One final test comparison was attempted. Subclutter visibility as defined by Skolnik in Reference 2, was measured to be 19 dBm for the AN/UPS-1D with delay-line canceler, and 21 dBm with the range-gated MTI system. The results of the range-gated MTI test are shown in Figures 25 and 26. With the facilities and test equipment available no practical means of measuring MTI improvement factor was possible. A practical method to measure this factor would certainly offer a more precise performance figure of merit than the subclutter visibility measurement.

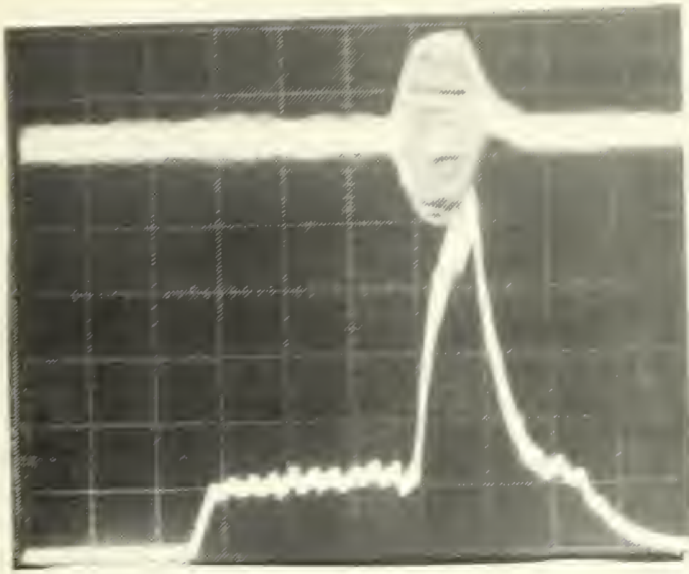

Bipolar video
(moving tgt.) and
positive video
(fixed tgt.) with
a vertical scale of
0.5 v/cm

Horizontal scale is
2 microseconds/cm

RGF MTI system
response with a
vertical scale of
2 v/cm

Figure 25. Range-gated MTI system response to simutaneous fixed and moving targets of equal amplitude and coincident in range (time).

Bipolar video
(at -21 dBm)
and fixed tar-
get video (at
0 dBm)

(same scales
as Figure 25)

RGF MTI system
response

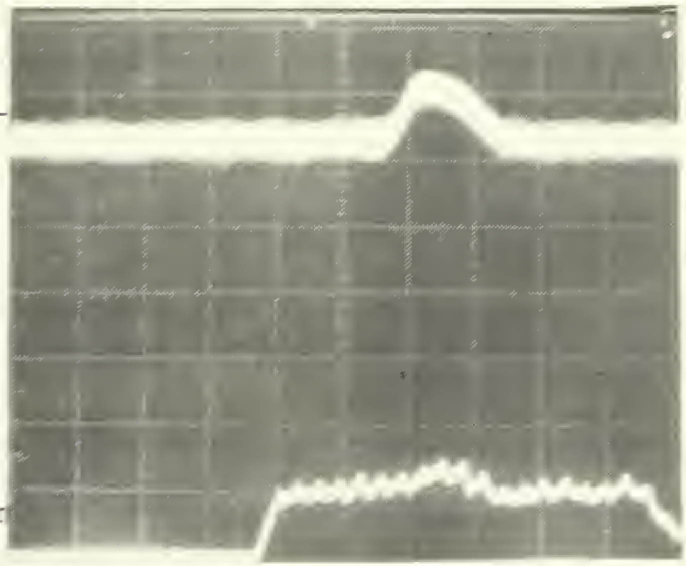

Figure 26. Range-gated MTI system response when the moving target of Figure 20 is -31 dBm (with respect to the fixed target of Figure 20).

VII. EXTENDABILITY

Extendability of the system has been provided by constructing the circuits on plug-in circuit boards. Future improvements and simplifications may be incorporated by modifying and/or replacing individual components, circuits, or circuit boards. Additional channels may be incorporated by adding additional circuit boards and shift registers if more than 20 channels are desired.

For a complete MTI processor with many more than 20 channels, and multiple copies of the radar systems, special-purpose integrated circuits could be constructed to perform the various functions. Large scale integration (LSI) techniques could be applied here to significantly reduce the cost, size and power consumption.

Some areas of further study and improvement would be to increase the amount of jitter (while maintaining an average basic PRF) to further eliminate blind speeds, to redesign the sample-and-hold circuit utilizing integrated circuits, to design a circuit for full-wave rectification of the filtered signal in the video reconstructor and to use integrated circuits for the actual video reconstruction with a modification to eliminate that part of the pedestal from the MTI system video output not associated with noise.

Other areas for improvement would be to design wideband video amplifiers and a digital delay circuit, construct them on circuit boards and interface them with the RGF processor. This change would eliminate the Hewlett and Packard video amplifiers and the Tektronix 546 oscilloscope in Figure 12 (Range-gated MTI test set-up).

VIII. CONCLUSIONS

As previously stated, several successful MTI systems employing range-gated filtering and timing circuits have been constructed and tested. The purpose of this work was to improve, simplify and modify an existing range-gated system [Ref.1]. The goals were to eliminate blind speeds, increase the effectiveness of the range-gated bandpass channel filters and reduce the minimum discernable signal of the system.

New timing circuitry allowed operation in a jittered PRF mode, thus acheiving almost total elimination of blind speeds, the exception being those targets with radial velocities close to 180 knots. However these targets do have a good probability of detection as discussed in Section VII. The circuits can easily be extended for a larger number of channels. The extensive use of integrated circuits was particularly helpful in achieving low cost, small size, and simplicity.

Comparison of the improved range-gated channels with the previously constructed circuits showed that considerable simplification due to a reduction in the number of components and physical size has been accomplished. The primary area of simplification and size reduction is the bandpass filters which have been reduced from eight transistors and 38 resistors and capacitors to one integrated circuit, four resistors and one capacitor. Each new filter circuit occupies approximately one-half of the circuit board area and yields a 15 dB improvement in the band-reject region of the filter frequency response. This considerable improvement was the primary reason that there was a 3.1 dB reduction in the minimum discernable signal

compared to Koral's [Ref.1]. MTI system and a 4 dB reduction compared to the AN/UPS-1D's delay-line canceler MTI system.

Thus the results were considered to be successful. They are also considered to be a good demonstration of the simplicity and effectiveness of MTI with range gates and filters.

APPENDIX A. TIMING CIRCUIT WAVEFORMS

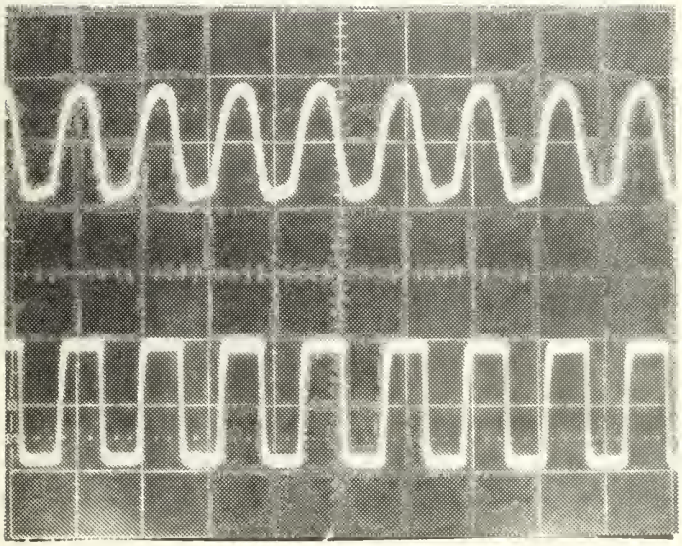

Vertical scale
2 v/cm

Horizontal scale
0.5 usec/cm

f_o 1.6128 Hz

Figure 27. Output of master oscillator (upper trace) and output of pulse shaper (lower trace).

Vertical scale
2 v/cm

Horizontal scale
1 usec/cm

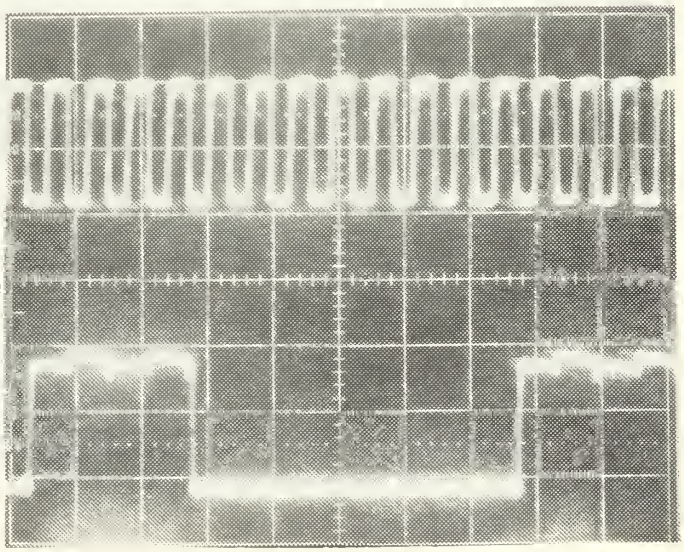

Figure 28. Clock pulses at f_o (upper trace) and f_o divided by 12 (lower trace).

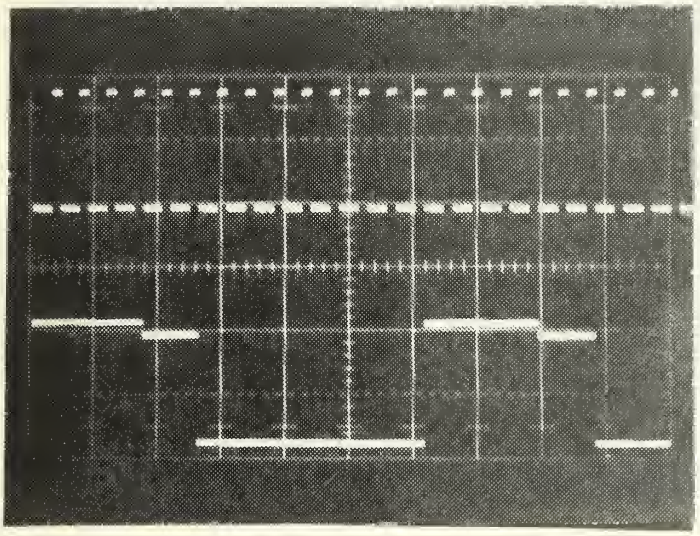

Vertical scale
2 v/cm

Horizontal scale
10 usec/cm

Figure 29. f_o divided by 12 (upper trace)
f_o divided by 144 (lower trace).

Vertical scale
2 v/cm

Horizontal scale
200 usec/cm

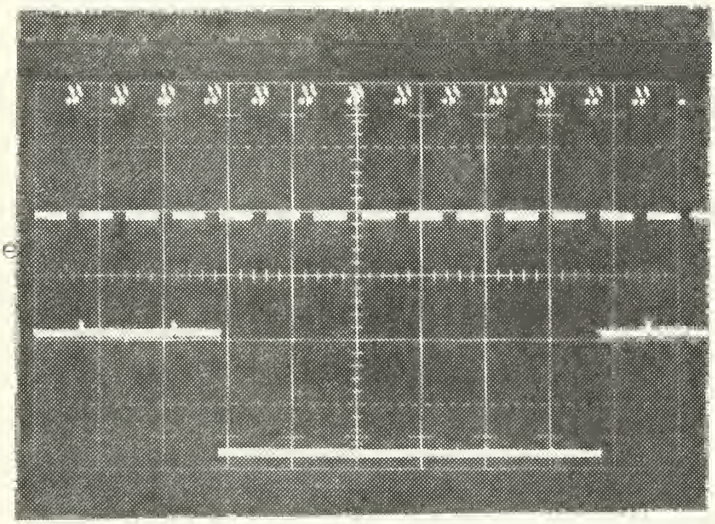

Figure 30. f_o divided by 144 (upper trace)
f_o divided by 2016 or 800 Hz
(lower trace).

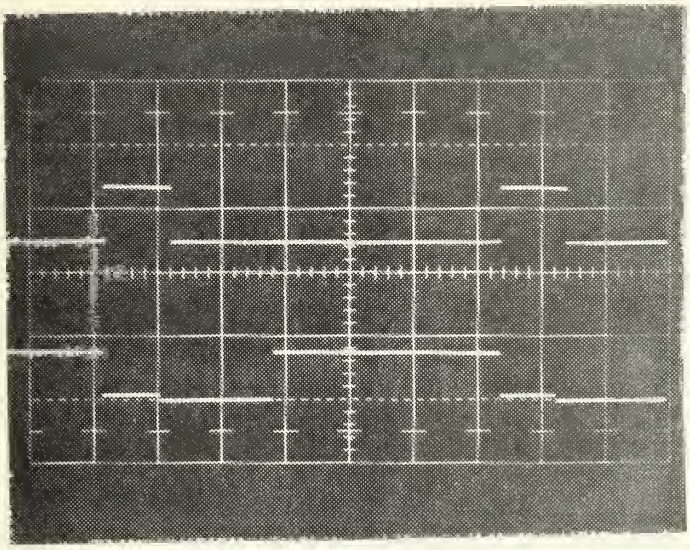

Vertical scale
5 v/cm

Horizontal scale
200 usec/cm

Figure 31. f_o divided by 2016 or 800 Hz (upper trace) output of 1st one-shot multi without PRF jitter (lower trace)

Vertical scale
5 v/cm

Horizontal scale
200 usec/cm

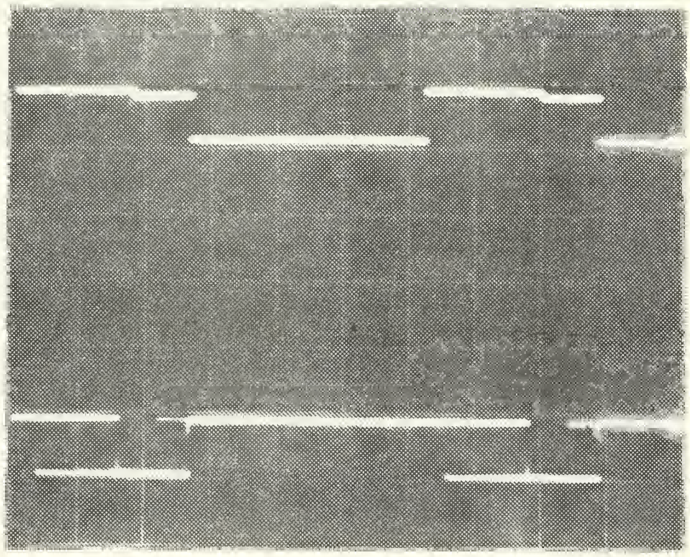

Figure 32. f_o divided by 2016 or 800 Hz (upper trace) output of 1st one-shot multi with PRF jitter (lower trace).

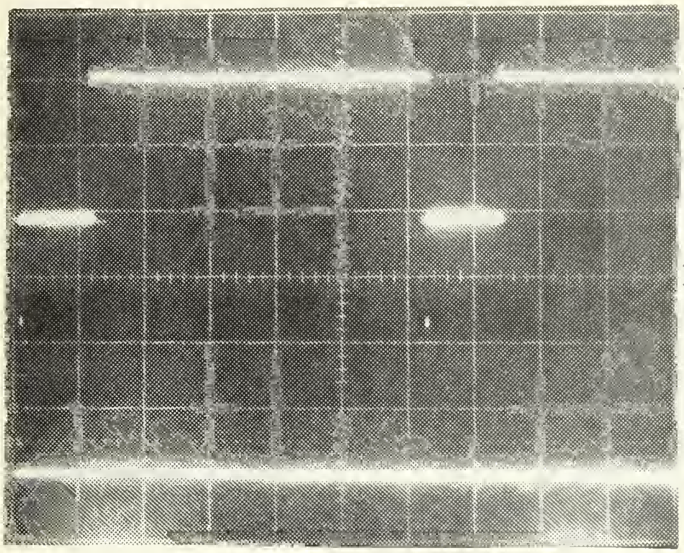

Vertical scale
2 v/cm

Horizontal scale
200 usec/cm

(w/o PRF jitter)

Figure 33. Output 1st one-shot multi (upper trace)
output 2nd one-shot multi (lower trace).

Vertical scale
2 v/cm

Horizontal scale
0.5 usec/cm

(w/o PRF jitter)

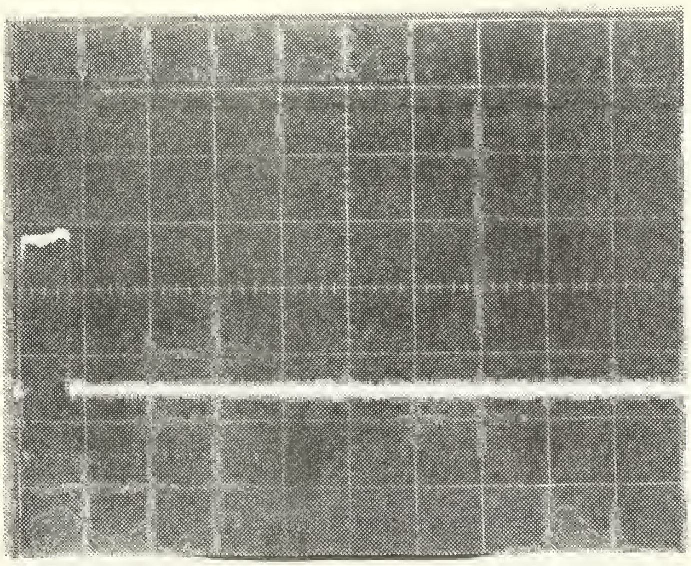

Figure 34. 0.5 usec pulse output of 2nd one-shot multi.

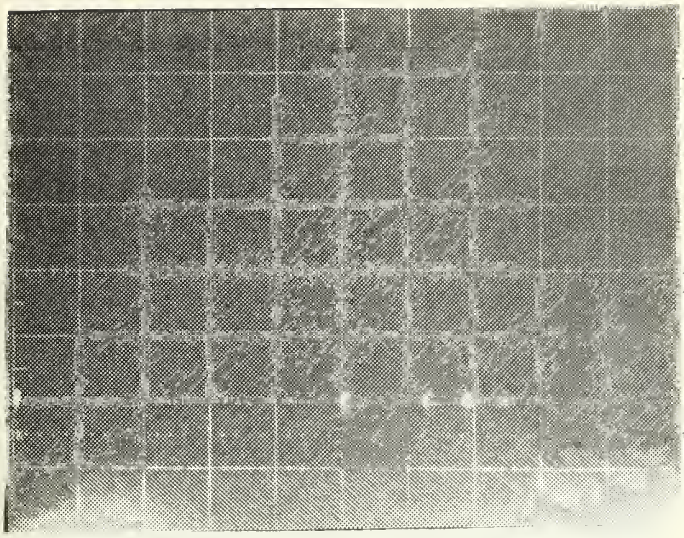

Vertical scale
2 v/cm

Horizontal scale
200 usec/cm

With 500 usec of
PRF jitter

Figure 35. Output and one-shot multi with PRF jitter applied.

Vertical scale
5 v/cm

Horizontal scale
200 usec

(f_j = 980 Hz)

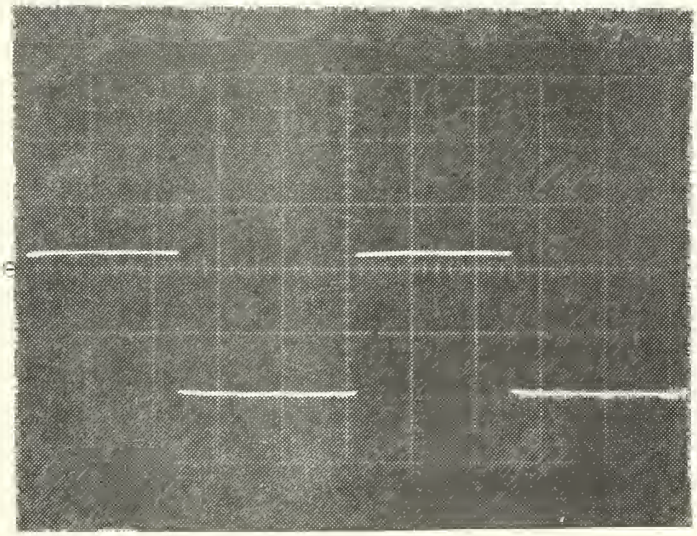

Figure 36. Jitter voltage applied to V_{cc} pin of 1st one-shot multi.

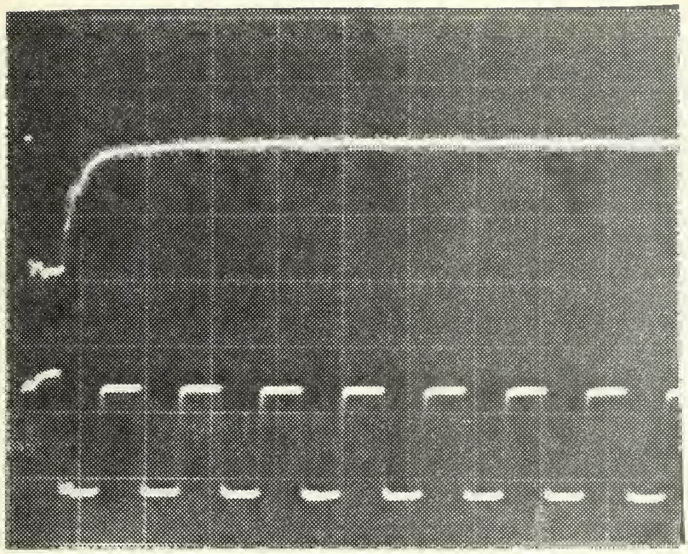

Vertical scale
2 v/cm

Horizontal scale
0.5 usec/cm

(w/o PRF jitter)

Figure 37. Output of clock and trigger synchronizer (upper trace). Clock pulses (lower trace).

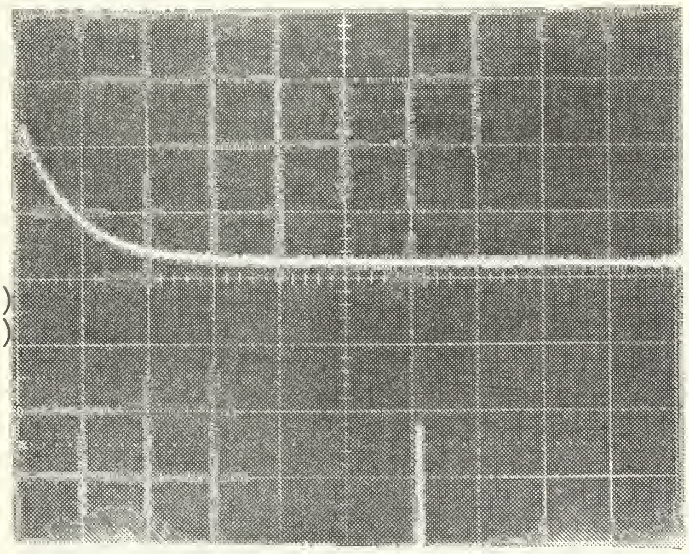

Vertical scale
10 v/cm

Horizontal scale
2 usec/cm (upper)
2 usec/cm (lower)

(w/o PRF jitter)

Figure 38. Radar trigger from transistor amplifier.

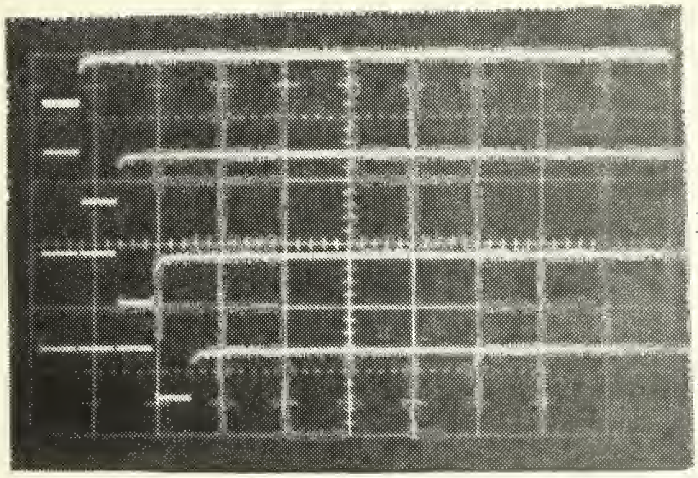

Vertical scale
5 v/cm

Horizontal scale
1 usec/cm

(w/o PRF jitter)

Figure 39. First four gating pulses from the shift registers to range-gate channels.

Vertical scale
10 v/cm

Horizontal scale
200 usec/cm

(approx. 500 usec of PRF jitter)

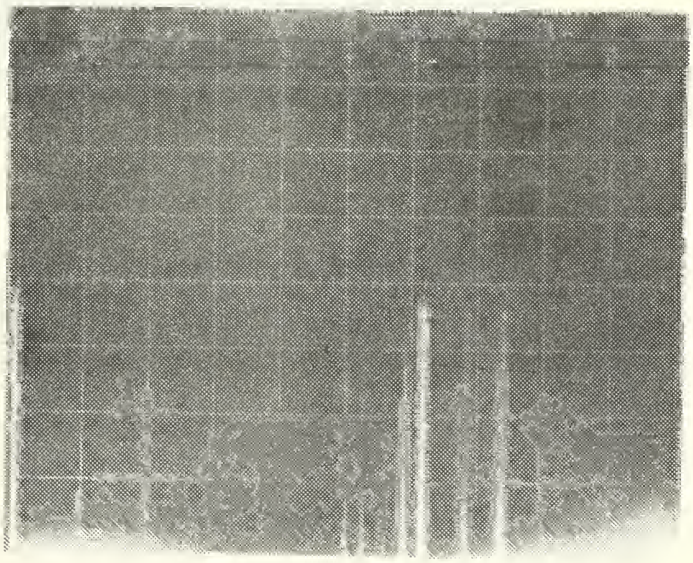

Figure 40. Jittered radar trigger from transistor amplifier.

Vert. scale
5 v/cm

Horiz. scale
0.5 usec/cm

Vert. scale
2 v/cm

Horiz. scale
200 usec/cm

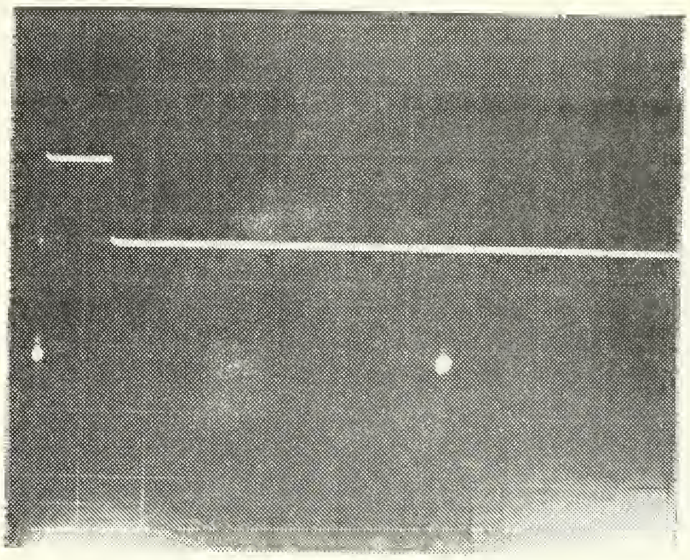

Figure 41. Reshaped trigger pulse from Systron-Donner pulse generator (without PRF jitter).

APPENDIX B. SINGLE CHANNEL WAVEFORMS

Input

Vert. scale
2 v/cm

Horiz. scale
2 msec/cm

Output

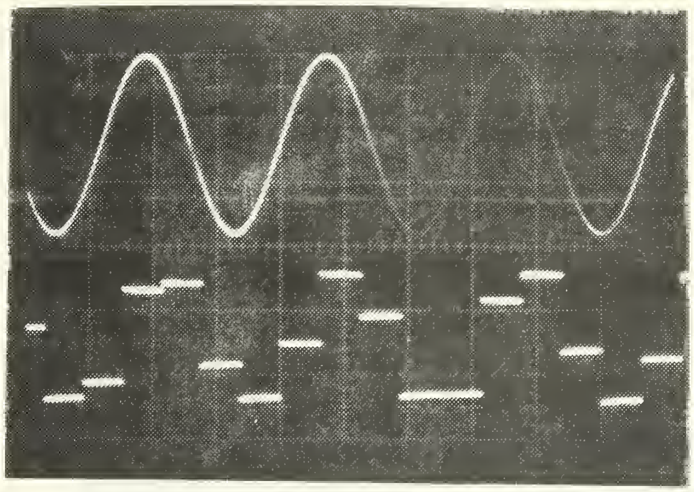

Figure 42. Sample-and-hold operation, one channel (200 Hz sine wave as input, no PRF jitter).

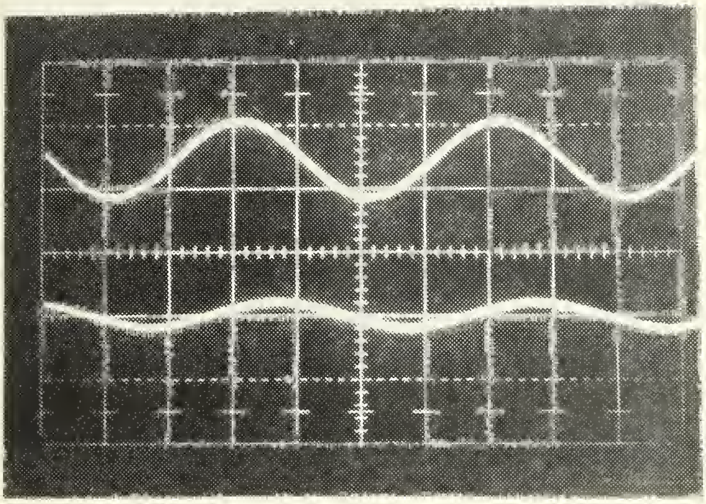

Input
(vert. scale
5 v/cm)

Output at -24 dBm
(vert. scale
0.5 v/cm)

Horiz. scale
5 msec/cm

Figure 43. Bandpass filter response to a 50 Hz sine wave input (no PRF jitter).

Input

Vert. scale
2 v/cm

Horiz. scale
5 msec/cm

Output

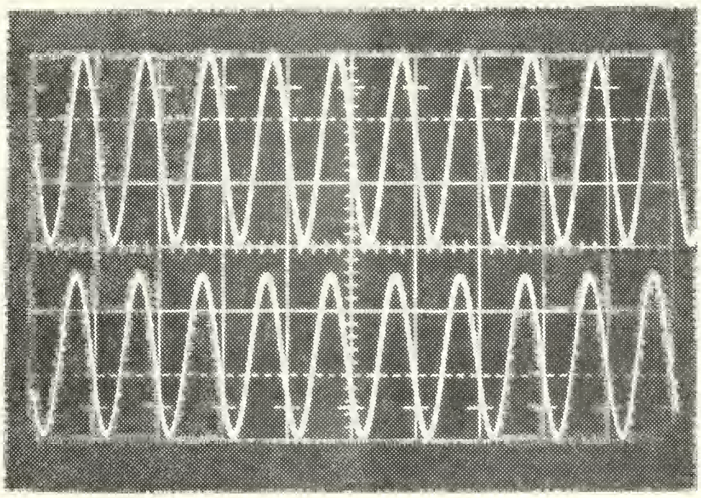

Figure 44. Bandpass filter response to a 200 Hz sine wave input (no PRF jitter).

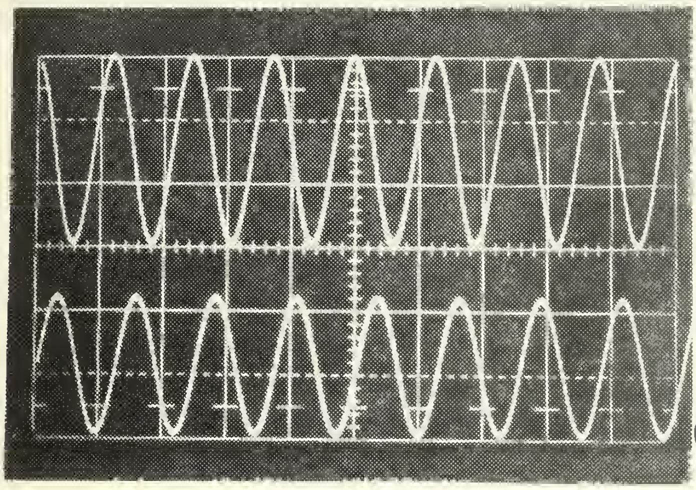

Input

Vert. scale
2 v/cm

Horiz. scale
2 msec/cm

Output

Figure 45. Bandpass filter response to a 400 Hz sine wave (no PRF jitter).

800 Hz Input
(vert. scale 5 v/cm)

Output
(vert. scale 0.5 v/cm)

1600 Hz Input
(vert. scale 5 v/cm)

Output
(vert. scale 0.5 v/cm)

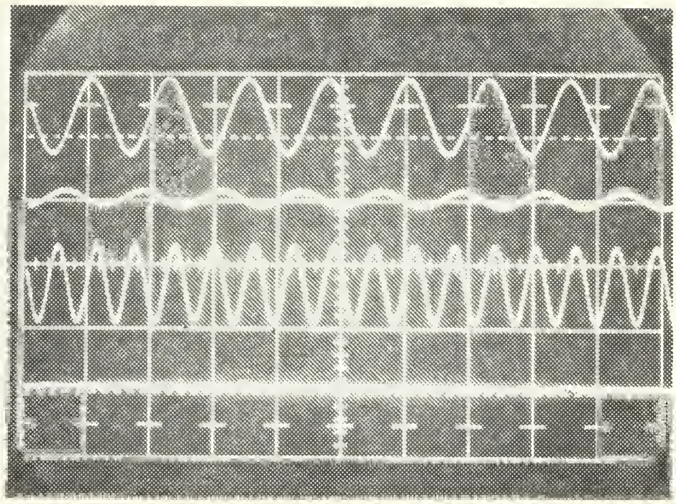

Figure 46. Bandpass filter response to 800 Hz and 1600 Hz sine waves (no PRF jitter).

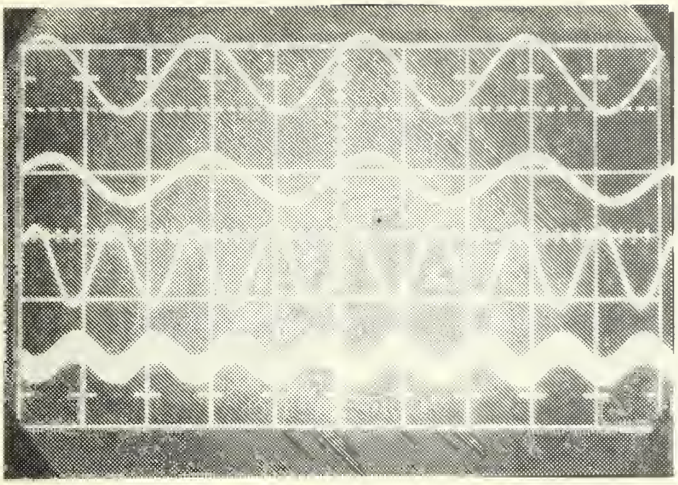

Figure 47. Sample-and-hold and filter response to 200 Hz and 400 Hz sine waves (no PRF jitter).

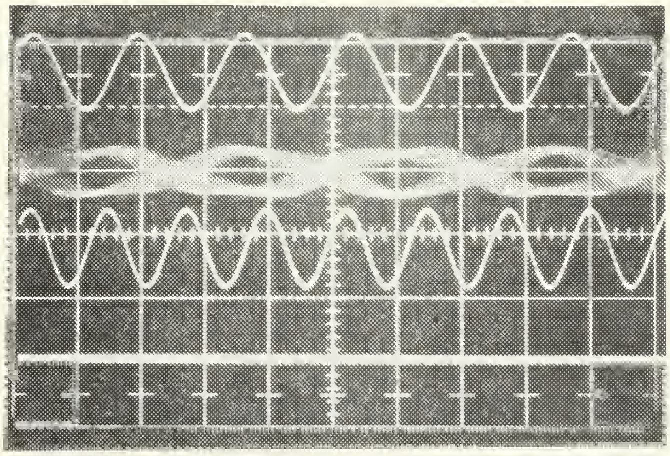

Figure 48. Sample-and-hold and filter response to 600 Hz and 400 Hz sine waves (no PRF jitter).

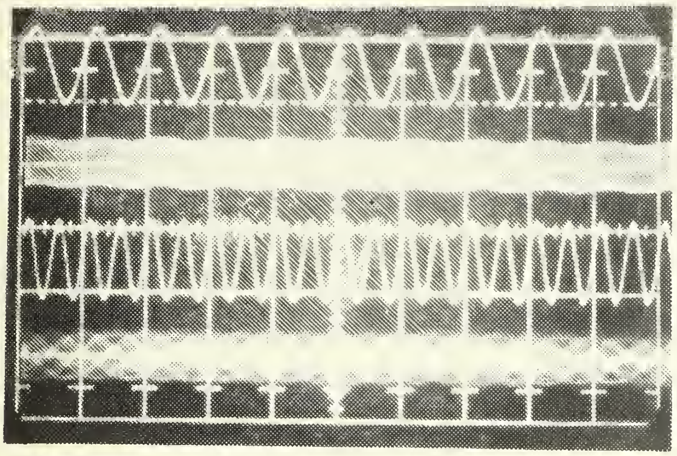

1000 Hz input to S&H

Output of filter

2000 Hz input to S&H

Output of filter

Vert. scale 5 v/cm
Horiz. scale
1 msec/cm

Figure 49. Sample-and-hold filter response to 1000 Hz and 2000 Hz sine waves (no PRF jitter).

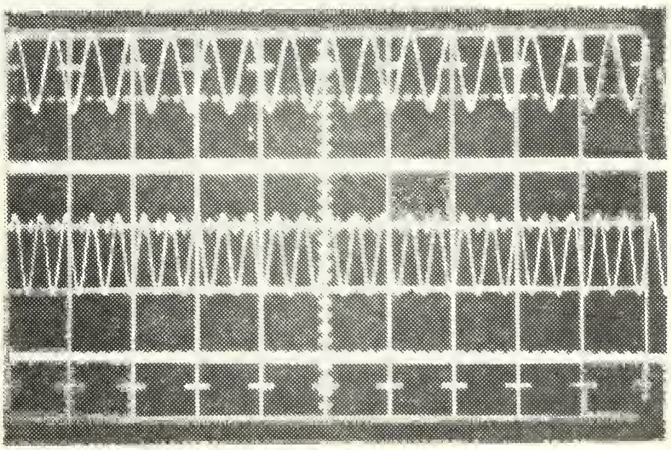

1600 Hz input to S&H

Output of filter

2400 Hz input to S&H

Output of filter

Vert. scale 5 v/cm
Horiz. scale
1 msec/cm

Figure 50. Sample-and-hold and filter response to 1600 Hz and 2000 Hz sine waves (no PRF jitter).

1. 5 KHz input to S&H

2. Output of filter

3. 10 KHz input to S&H

4. Output of filter

Vert. scale 5 v/cm
Horiz. scale 200 usec/cm

1
2
3
4

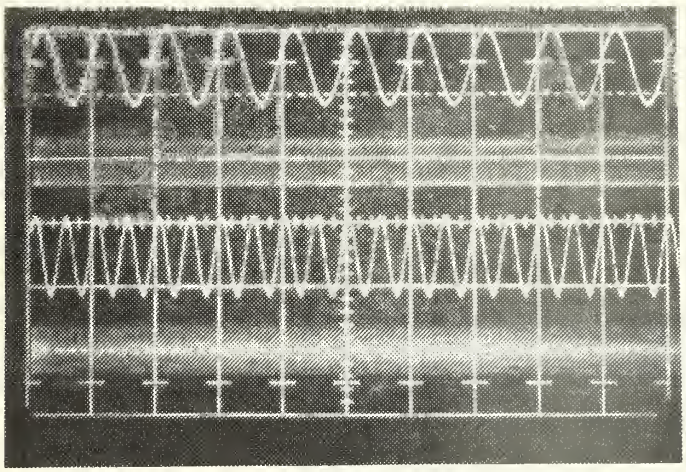

Figure 51. Sample-and-hold/filter response to 5 KHz and 10 KHz sine waves (no PRF jitter).

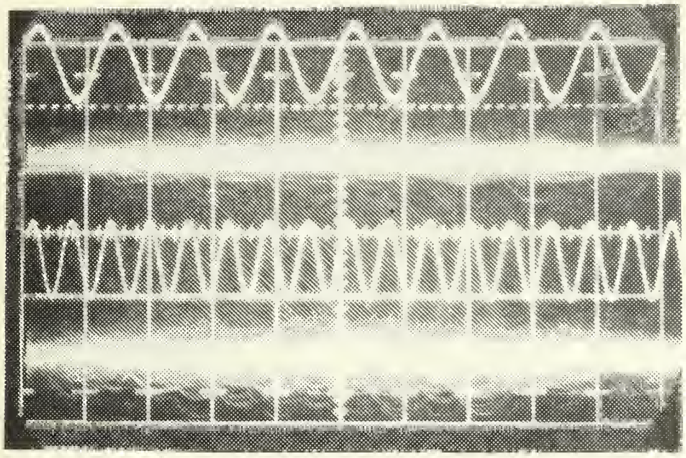

800 Hz input to S&H
(vert. scale 5 v/cm)

Output of filter
(vert. scale 2 v/cm)

1600 Hz input to S&H
(vert. scale 5 v/cm)

Output of filter
(vert. scale 2 v/cm)

Horiz. scale
1 msec/cm

Figure 52. Sample-and-hold/filter response to 800 Hz and 1600 Hz sine waves (with PRF jitter).

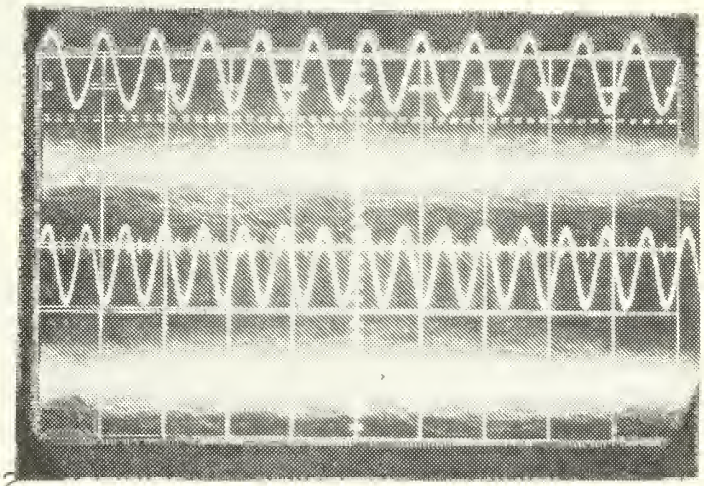

2400 Hz input to S&H

Output of filter

3200 Hz input to S&H

Output of filter

Same scales as Figure 52.

Figure 53. Sample-and-hold/filter response to 2400 Hz and 3200 Hz sine waves (with PRF jitter.

1. 4 KHz input to S&H (vert. scale 5 v/cm)

2. Output of filter (vert. scale 2 v/cm)

3. 4.8 KHz input to S&H (vert. scale 5 v/cm)

4. Output of filter (vert. scale 2 v/cm)

Horiz. scale 200 usec/cm

1

2

3

4

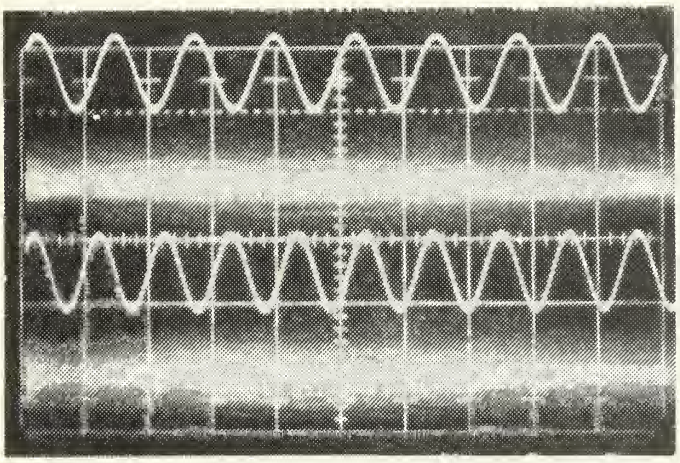

Figure 54. Sample-and-hold/filter response to 4 KHz and 4.8 KHz sine waves (with PRF jitter).

1. 200 Hz sine wave (no PRF jitter)
   (vert. scale 2 v/cm)

2. Output of detector (rectifier)
   in the Video reconstructor
   (vert. scale 0.5 v/cm)

Horiz. scale 2 msec/cm

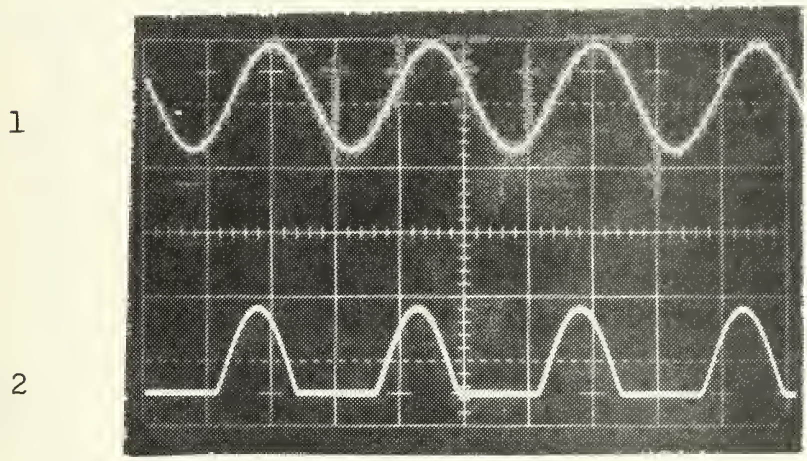

Figure 55. Detector output in the Video reconstructor circuit.

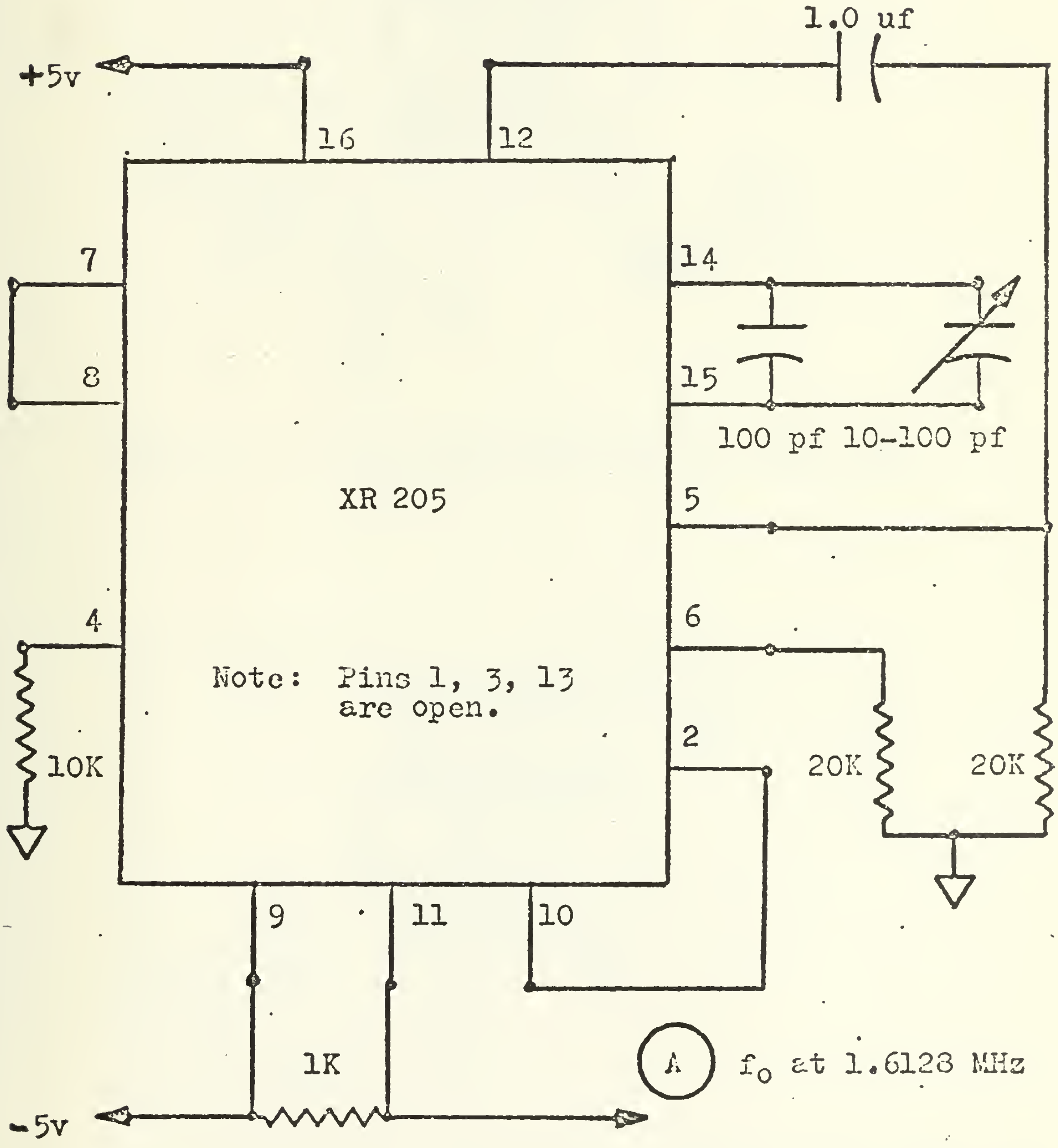

Figure 56. XR 205 Master oscillator (Ref. 5 & 7).

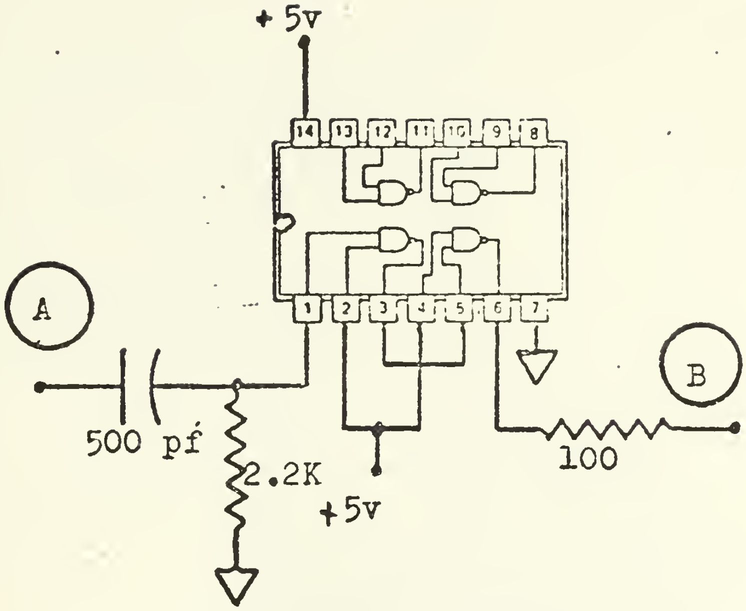

Figure 57. 7400 (NAND) pulse shaper (Ref. 6).

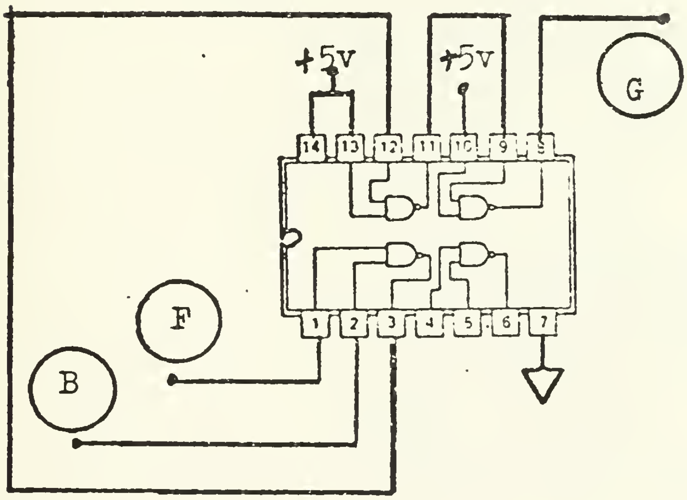

Figure 58. 7400 (NAND) clock/trigger synchronizer (Ref. 6)

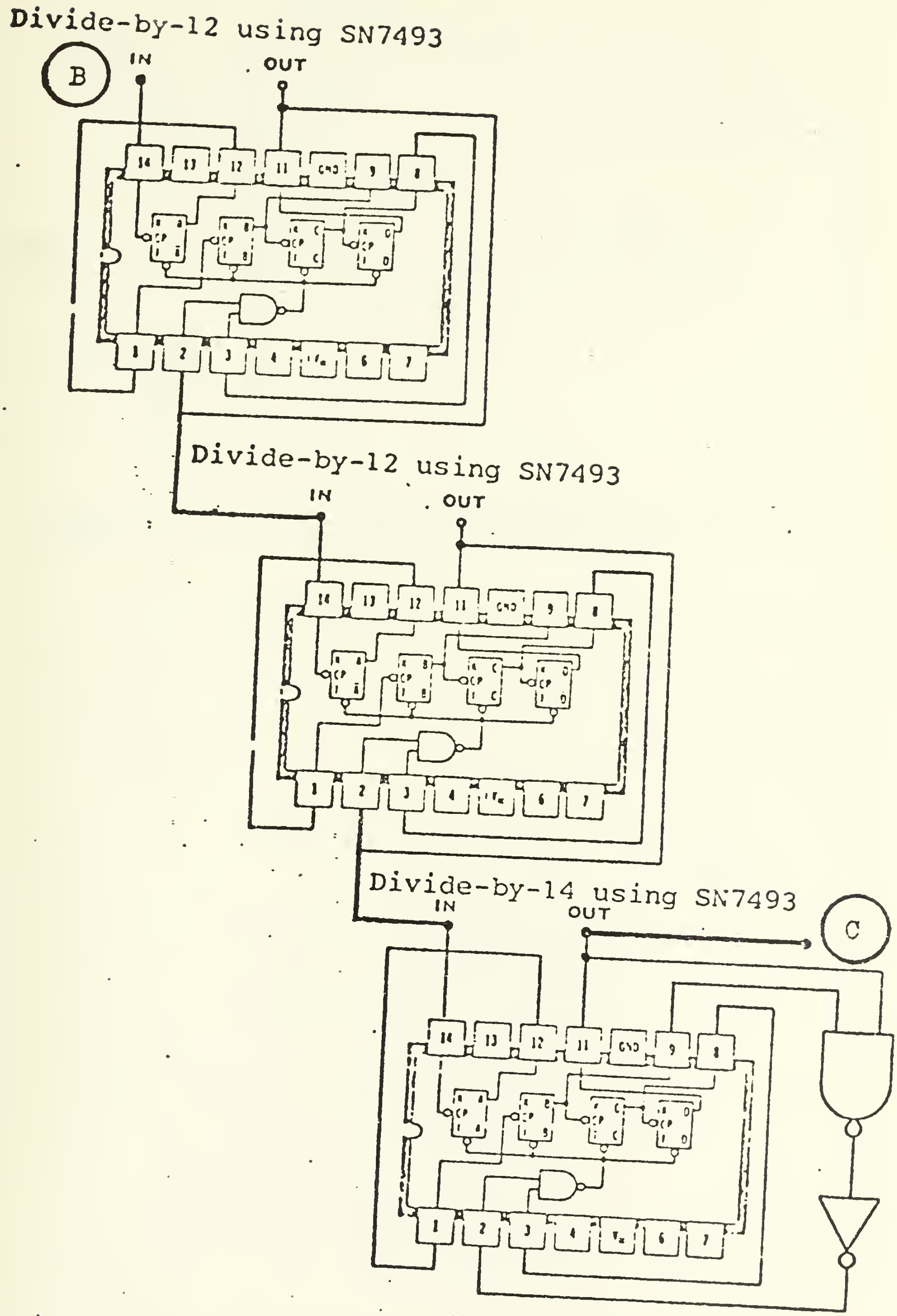

Figure 59. Frequency count down system (Ref. 5 & 6).

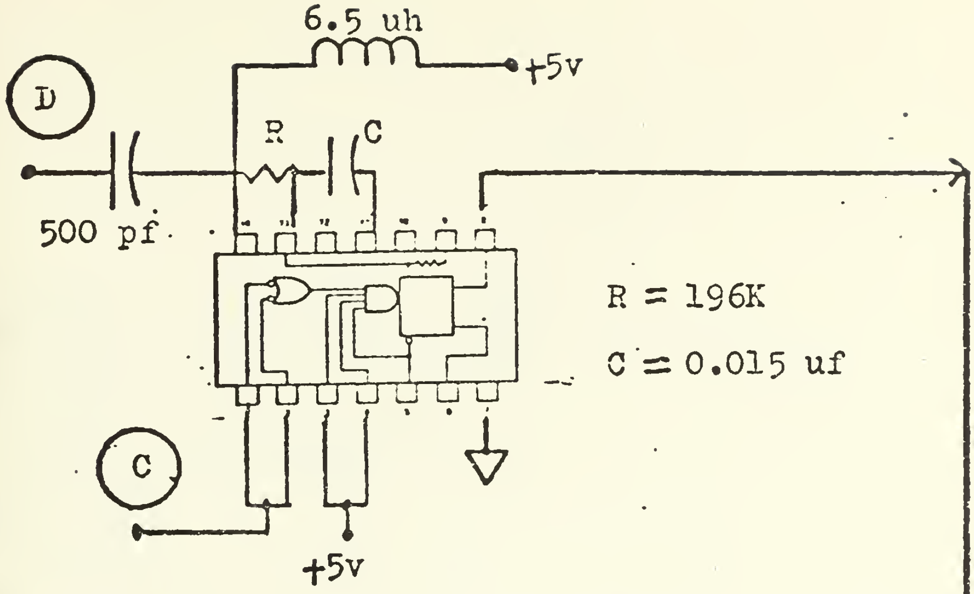

Figure 60. 74122 First one-shot multi. (Ref. 6)

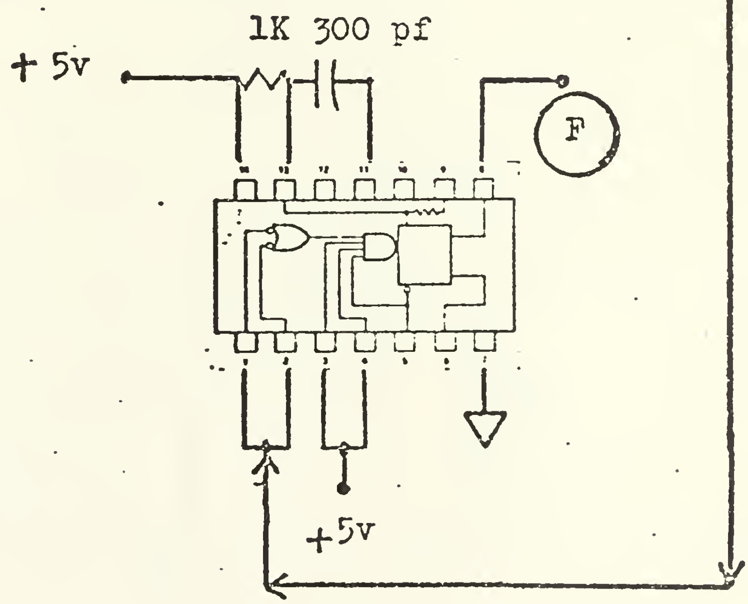

Figure 61. 74122 Second one-shot multi. (Ref. 6).

$$f_o = [2(V - V_c)] / [R_1 C_1 V]$$

f_o = 980 KHz

$V^+ = +24$; $V_c = +22.5v$

R_1 = 1.28K

C_1 = 0.1 uf

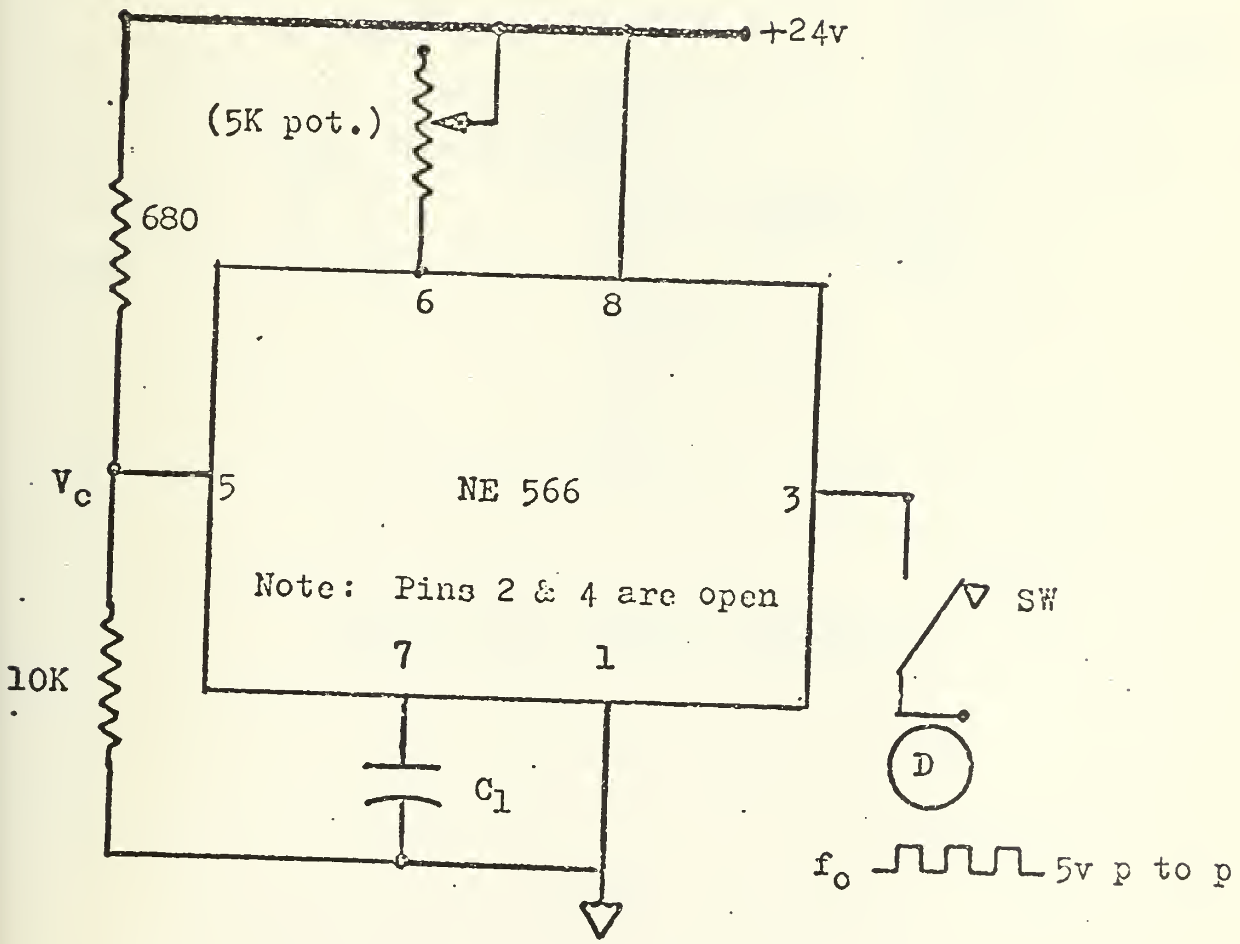

Figure 62. Jitter voltage generator (Ref. 5 & 6).

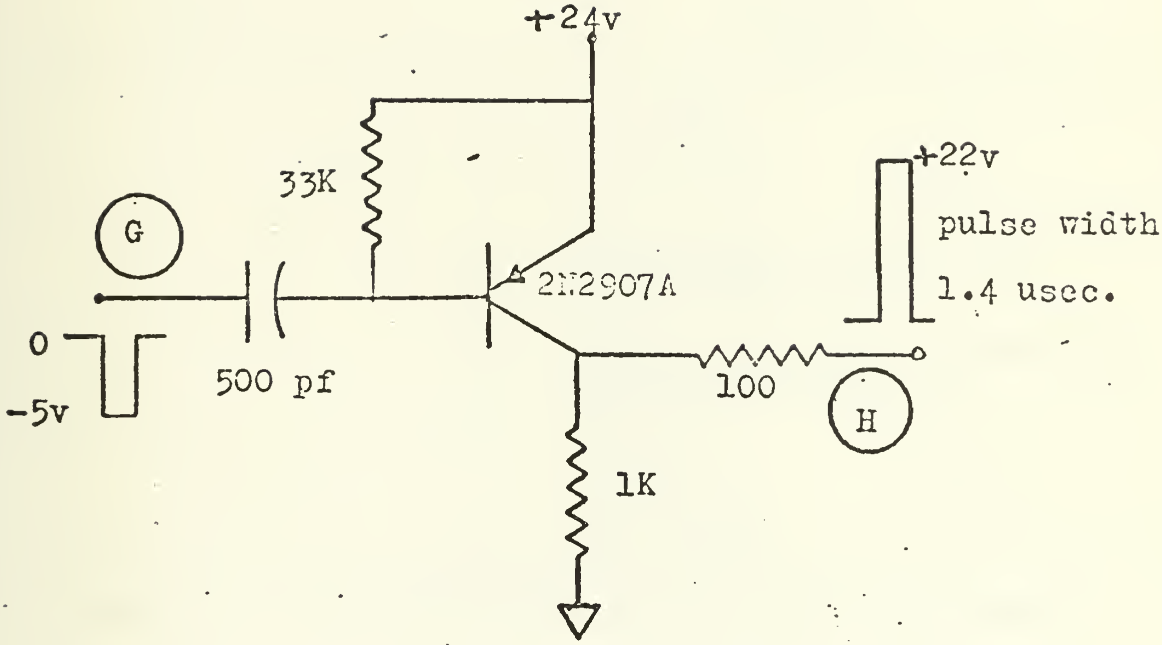

Figure 63. Trigger amplifier.

Pin	Function
1	-5 volts
5	+5 volts
11	Clock pulse output from B of Figure 57
13	Trigger to radar transmitter from H of Figure 63
20	Ground
22	+24 volts

Table II. Timing circuit board connection diagram.

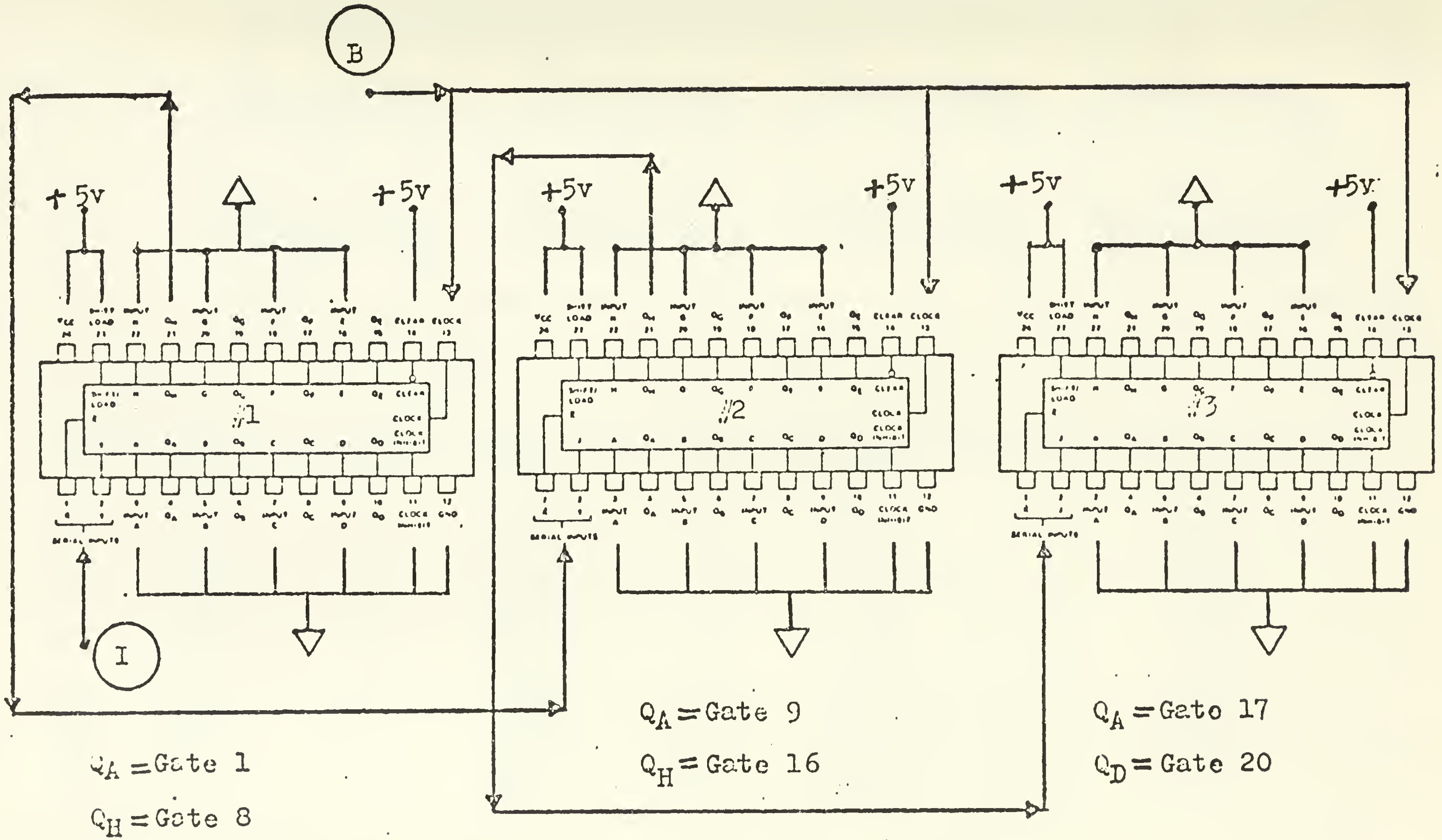

Figure 64. 74199 Shift registers (Ref. 1 & 6).

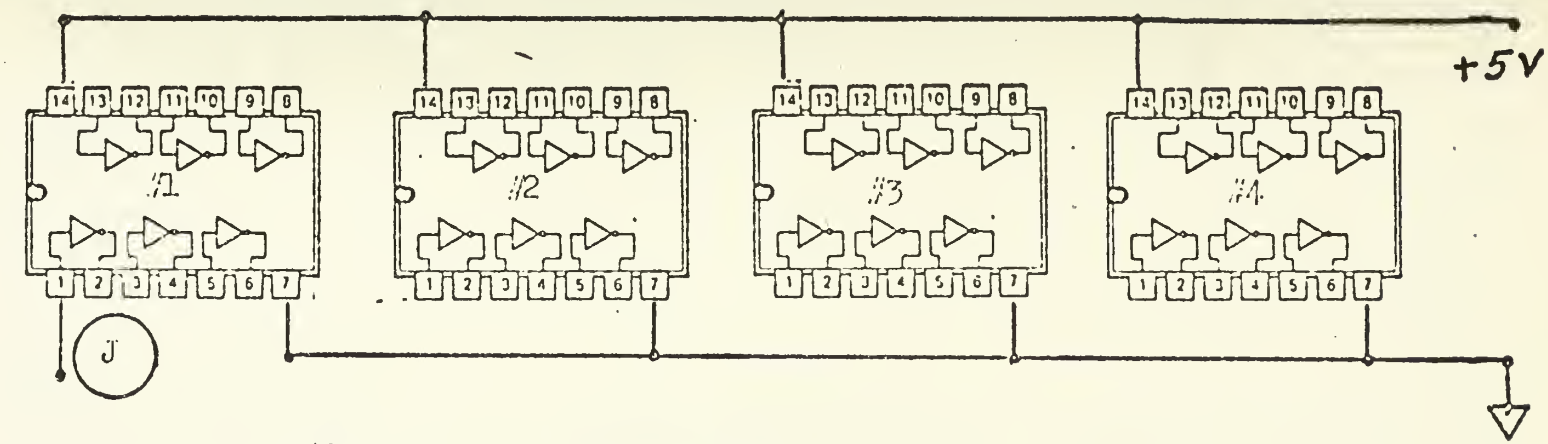

#1		#2		#3		#4	
Pin	Gate	Pin	Gate	Pin	Gate	Pin	Gate
1	1 in	1	4 in	1	11 in	1	17 in
2	1 out	2	4 out	2	11 out	2	17 out
3	2 in	3	9 in	3	12 in	3	18 in
4	2 out	4	9 out	4	12 out	4	18 out
5	3 in	5	10 in	5	open	5	open
6	3 out	6	10 out	6	open	6	open
8	7 out	8	14 out	8	open	8	open
9	7 in	9	14 in	9	open	9	open
10	6 out	10	13 out	10	16 out	10	20 out
11	6 in	11	13 in	11	16 in	11	20 in
12	5 out	12	8 out	12	15 out	12	19 out
13	5 in	13	8 in	13	15 in	13	19 in

Figure 65. 7404 Inverters (Ref. 6).

Range Gate	Pin
1	22
2	21
3	20
4	19
5	18
6	17
7	16
8	15
9	14
10	13
11	12
12	11
13	10
14	9
15	8
16	7
17	6
18	5
19	4
20	3

Pin 2 Clock pulses from B Figure 57

Pin 1 Delayed trigger from Systron-Donner pulse generator to (provide serial data input) load 1st shift register

Table III. Shift register/inverter circuit board connection diagram.

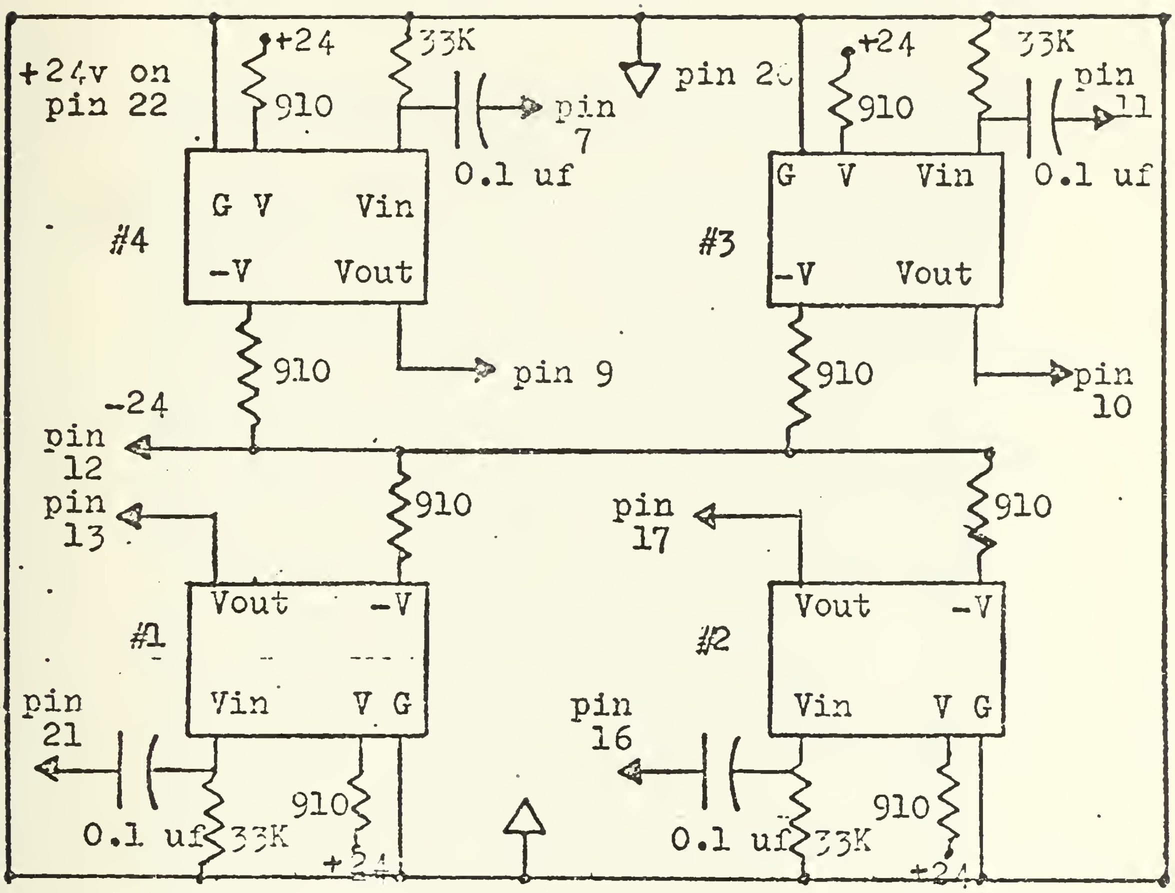

SPECIFICATIONS

Transfer characteristics — Butterworth,
Gain in pass-band — 0 db ± .2db
Cut-off frequency accuracy — ± 2% @ − 3 db
Maximum input voltage — 10 volts peak.
Supply voltage — ± 15 volts min., ±18 volts max.
DC drift — 20uV/°C typical.
Temperature range — 0°C to 70°C
(on request).
Temperature/Coefficient — .03%/°C.
Power consumption — 400 MW Max.

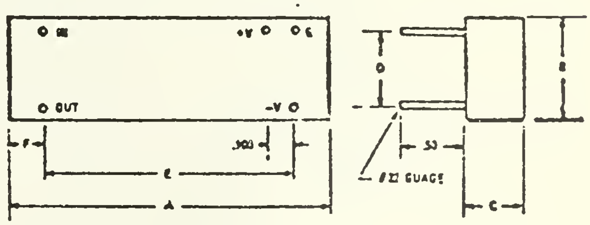

Dimensions (inches)					
A	B	C	D	E	F
2.00	1.00	.50	.600	1.100	.50

Figure 66. Bandpass filter specifications and connection diagram (Ref. 8).

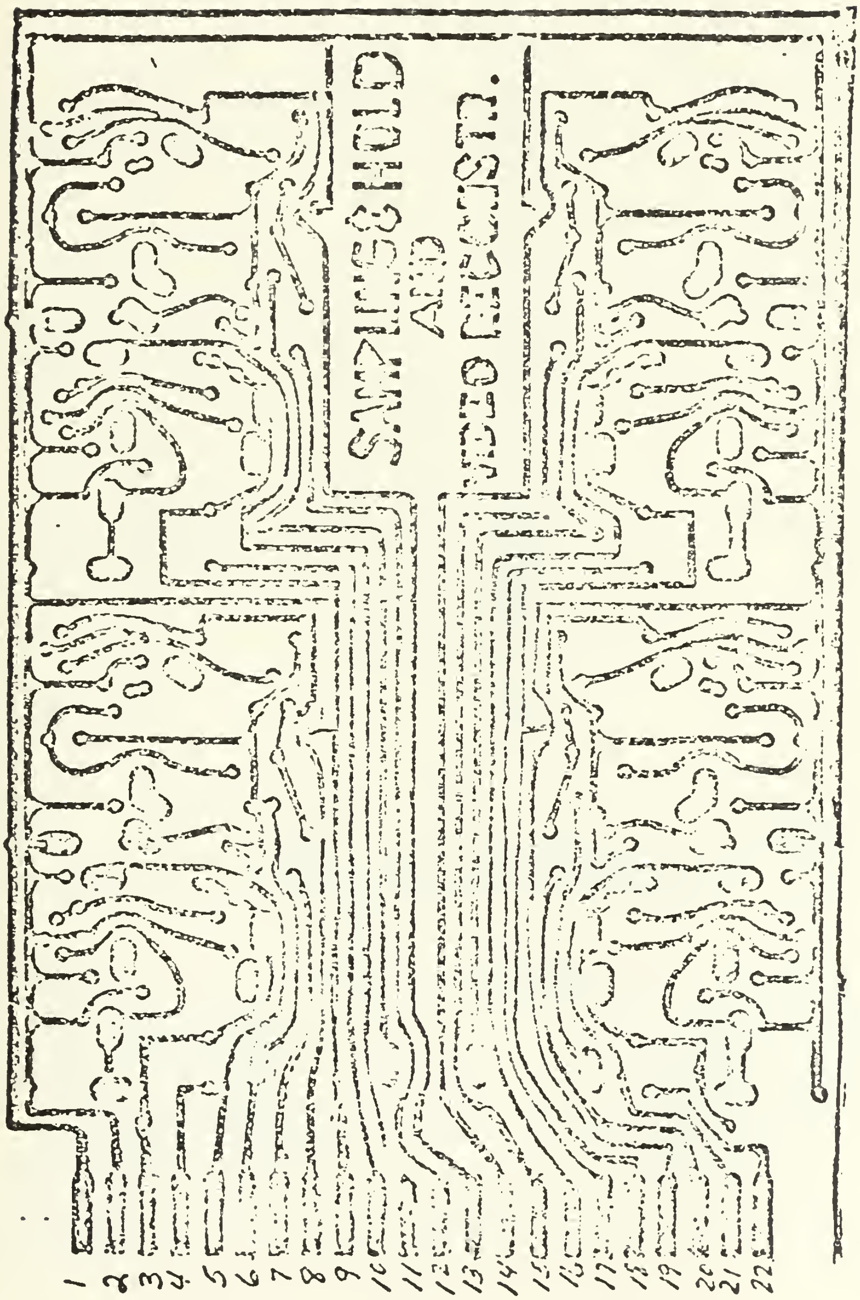

Figure 67. Printed circuit diagram of sample-and-hold/video reconstructor (Ref. 1)

Channels	Pin	Function
1, 5, 9, 13, 17	1*	a
" "	4	b
" "	5	c
" "	6	d
" "	7	e
" "	8	f
2, 6, 10, 14, 18	10	b
" "	10*	d
" "	11	c
" "	11*	a
" "	12	e
" "	13	f
3, 7, 11, 15, 19	12*	a
" "	13*	d
" "	14	f
" "	15	e
" "	16	c
" "	17	b
4, 8, 12, 16, 20	14*	d
" "	19	f
" "	20	e
" "	21	c
" "	22	b
" "	22*	a
		g
		h

Table IV. S&H/video reconstructor circuit board connection diagram.

Function I.D.
- a. 6K Potentiometer
- b. Video to S&H
- c. Output of S&H
- d. Gating pulse in
- e. Filtered video in
- f. MTI video out
- g. 24v
- h. Ground

Notes:
1. 1* Pin 1 top only
   1 Pin 1 bottom only
2. All function b's jumped together
3. All function f's jumped together

LIST OF REFERENCES

1. Koral, N., Radar Range-Gated MTI Processor, Master's Thesis Naval Postgraduate School, Monterey, December 1972.
2. Skolnik, M. I., Introduction to Radar Systems, pp. 113-163, McGraw-Hill Book Company, Inc., 1962.
3. Skolnik, M. I., Radar Handbook, pp. 35.1-35.10, McGraw-Hill, 1970.
4. Oppenheim, A. V. and Schafer, R. W., Digital Signal Processing, pp. 27-30, Prentice-Hall, Inc., 1975.
5. Cazes, J., Integrated Circuits Applications and Experiments That Can Be Performed on the Op-Amp Designer--model 2, E and L Instruments, Inc., Derby, Conn., 1974.
6. Signetics, Integrated Circuits Catalogue for Digital/Linear/MDS Devices, pp. 2.1-2.3, pp. 2.9-2.10, pp. 2.100-2.101, pp. 2.116-2.118, pp. 2.180-2.182, 1972.
7. R-OHM, Specification for XR-205 Monolithic Waveform Generator, June 1974.
8. Data Delay Devices, Specification for DIP Active Filter, June 1975.

INITIAL DISTRIBUTION LIST

		No. Copies
1.	Defense Documentation Center Cameron Station Alexandria, Virginia 22314	2
2.	Library, Code 0212 Naval Postgraduate School Monterey, California 93940	2
3.	Department Chairman, Code 52 Department of Electrical Engineering Naval Postgraduate School Monterey, California 93940	1
4.	Professor D. B. Hoisington, Code 52Hs Department of Electrical Engineering Naval Postgraduate School Monterey, California 93940	1
5.	Radar Laboratory Department of Electrical Engineering Naval Postgraduate School Monterey, California 93940	1
6.	Naval Research Laboratory, Code 5305 Washington, D. C. 20375	1
7.	Capt. Charles J. Boyle, USMC 182-30-7859 Marine Corps Tactical System Support Activity Marine Corps Base, Camp Pendleton California 92055	1

Thesis 163603
B7954 Boyle
c.1 Improved radar range-
gated MTI processor.